

**LAKE SEDIMENT ARCHIVES OF ATMOSPHERIC POLLUTION FROM THE
PERUVIAN AND BOLIVIAN ANDES**

by

Colin A. Cooke

B.A., University of Alberta, 2003

Submitted to the Graduate Faculty of
Arts and Sciences in partial fulfillment
of the requirements for the degree of
Master of Science

University of Pittsburgh

2006

UNIVERSITY OF PITTSBURGH
FACULTY OF ARTS AND SCIENCES

This thesis was presented

by

Colin A. Cooke

It was defended on

June 15, 2006

and approved by

Charles Jones, Ph.D., Lecturer

Michael Rosenmeier, Ph.D., Assistant Professor

Thesis Director: Mark Abbott, Ph.D., Assistant Professor

Copyright © by Colin A. Cooke

2006

LAKE SEDIMENT ARCHIVES OF ATMOSPHERIC POLLUTION FROM THE PERUVIAN AND BOLIVIAN ANDES

Colin A. Cooke, M.S.

University of Pittsburgh, 2006

Despite a richly-documented history of metallurgy following Hispanic conquest of the Inca, little is known concerning the loci and intensities of earlier metallurgical activities. Lake sediments offer one strategy to reconstruct this history because the deposition of trace elements associated with smelting form a continuous archive that can be assessed in the context of regional archaeology.

To reconstruct regional histories of late Holocene atmospheric pollution, two lake sediment cores were collected from mining areas in the central Peruvian Andes. Lake sediment stratigraphies of elemental concentrations and isotopic ratios preserve a regional record of pre-Incan, Incan, and Colonial smelting practices. Our records provide the first evidence for intensive, pre-Colonial smelting in the central Peruvian Andes, and corroborate earlier findings from Bolivia. Surprisingly, smelting appears to have operated independent of oversight from the Wari (500 to 1000 AD) or Inca (1460 to 1532 AD) Empires. With Spanish arrival, smelting activity increased dramatically, only to be superseded by post-industrial pollution.

The two central Andean records were compared to two Bolivian records of atmospheric pollution. Initial Pb enrichment in Bolivia occurs contemporaneously with records from Peru ca. 400 AD. In Bolivia, this coincides with the expansion of the Tiwanaku Empire (ca. 400 to 1000 AD). Inca expansion across both Peru and Bolivia (~1450 AD) led to increased metallurgical activity at all four study sites. Our findings demonstrate the usefulness of paleolimnological

methods for reconstructing the timing and magnitude of smelting activity throughout the New World, and thus contribute directly to a fragmentary archaeological record.

TABLE OF CONTENTS

TABLE OF CONTENTS	VI
LIST OF TABLES	VIII
LIST OF FIGURES	IX
ACKNOWLEDGEMENTS	XI
1.0 INTRODUCTION.....	1
1.1 PRE-COLONIAL METALLURGY IN THE ANDES.....	1
1.2 SMELTING IN THE ANDES	2
2.0 1500 YEARS OF METALLURGY RECORDED BY LAKE SEDIMENTS FROM THE CENTRAL PERUVIAN ANDES.....	5
2.1 INTRODUCTION	5
2.2 STUDY SITES	7
2.3 METHODS.....	12
2.3.1 Core collection and chronology	12
2.3.2 Geochemical characterization.....	13
2.3.3 Lead isotopes	15
2.4 RESULTS.....	16
2.4.1 Core chronology	16
2.4.2 Core geochemistry	20
2.4.3 Data preparation.....	26
2.4.4 Isotopic contribution.....	26
2.5 DISCUSSION.....	28
2.5.1 Pre-Colonial and Colonial metal pollution.....	28
2.5.2 The modern era.....	36
2.6 CONCLUSION	36

3.0	LATE HOLOCENE HISTORIES OF ATMOSPHERIC LEAD DEPOSITION FROM THE CENTRAL ANDES: INSIGHT INTO PRE-HISPANIC METALLURGY ...	38
3.1	INTRODUCTION	38
3.2	STUDY SITES	39
3.3	METHODS.....	42
3.3.1	Core collection and chronology	42
3.3.2	Lead geochemistry	45
3.4	RESULTS	46
3.5	DISCUSSION.....	50
3.5.1	The Middle Horizon (~500 to 1000 AD).....	50
3.5.2	The Late Intermediate Period (~1000 to 1450 AD).....	52
3.5.3	The Late Horizon (~1450 to 1530 AD)	53
3.5.4	The Colonial era (1532 to 1900 AD)	54
3.6	CONCLUSION	55
4.0	THESIS CONCLUSION	57
4.1	FUTURE RESEARCH.....	57
APPENDIX A.....		59
TABLE OF LAKES STUDIED.....		59
APPENDIX B		60
ELEMENTAL CONCENTRATION DATA		60
BIBLIOGRAPHY.....		75

LIST OF TABLES

Table 2.1	Limnological parameters for the study lakes.....	12
Table 2.2	Instrument detection limits (IDL) and analytical error (1σ) for all elements measured from study sites. IDL and 1σ error are reported as $\mu\text{g g}^{-1}$ dry sediment mass.....	15
Table 3.1	Location of study sites and lake characteristics.....	39
Table 3.2	Table of ^{14}C dates used in this study.....	44

LIST OF FIGURES

- Figure 2.1 Map of Peru showing lake study sites (*italics*), archaeological sites and towns discussed in text. 9
- Figure 2.2 Base map of Laguna Chipian and the Cerro de Pasco area. 10
- Figure 2.3 Photos of Laguna Chipian (a and b), a presumed smelter and patio (c) and a large grinding wheel (d). The smelter and grinding wheel are located within the valley below the lake and are presumed to be colonial in age. 10
- Figure 2.4 (a) Base map of Laguna Pirhuacocha and the Morococha mining area. (b) Photo looking west-southwest showing coring location and the direction of outflow. 11
- Figure 2.5 Down-core sediment ^{210}Pb activities, composite age-depth models and bulk density profiles for (a) Laguna Chipian and (b) Laguna Pirhuacocha. Only those dates obtained on charcoal were used to construct age-depth models (see text). Error bars represent the 2σ error range on dates; error bars not shown are smaller than the data points displayed. 18
- Figure 2.6 Geochemical and isotopic stratigraphies and associated ^{210}Pb and ^{14}C dates for Laguna Chipian. All elemental concentrations are reported as $\mu\text{g g}^{-1}$ dry sediment mass. Analytical error bars are smaller than the data points shown. Two separate plots of Pb are shown to highlight smaller enrichments deeper in the core. Published $^{206}\text{Pb}/^{207}\text{Pb}$ isotopic ratios of Cerro de Pasco ore from Mukasa *et al.* (1990) and Sangster *et al.* (2000). 21
- Figure 2.7 Geochemical and isotopic stratigraphies and associated ^{210}Pb and ^{14}C dates for Laguna Pirhuacocha. Note the two separate plots of Ag, with the second plot omitting circled data points and top 5 cm. Also note the two plots for Pb using different scales, and the omission of the top 5 cm of data for Pb, Ag, Cu, Bi, and As in order to highlight trends down-core. The omitted data are shown separately in Figure 2.8. All elemental concentrations are reported as $\mu\text{g g}^{-1}$ dry sediment except for S, which is in mg g^{-1} . Published

$^{206}\text{Pb}/^{207}\text{Pb}$ isotopic ratios of Cerro de Pasco ore from Gunnesch <i>et al.</i> (1990) and Macfarlane <i>et al.</i> (1990).....	24
Figure 2.8 Industrial era geochemical histories for the last 150 years from (a) Laguna Chipian and (b) Laguna Pirhuacocha plotted against the ^{210}Pb chronologies.....	25
Figure 2.9 (a) Laguna Pirhuacocha elemental flux and $^{206}\text{Pb}/^{207}\text{Pb}$ ratios versus (b) archaeological reconstruction of regional cultural chronology. Periods of metal enrichment are synchronous with social stability in the region as indicated by the archaeological record, suggesting local or regional control of resources. The heavy black line in the Ag profile represents a five-point running average.....	30
Figure 2.10 (a) Laguna Chipian elemental flux and $^{206}\text{Pb}/^{207}\text{Pb}$ ratios versus (b) regional cultural chronology. After 1000 AD, qualitative trends in metal enrichment at Laguna Chipian correlate to those observed at Laguna Pirhuacocha, suggesting both locations are locally administered.....	33
Figure 3.1 Map of study lakes (<i>italics</i>) as well as archaeological sites and towns discussed in text. Arsenic-rich polymetallic orebodies as well as tin-rich ore deposits are noted on the map.....	40
Figure 3.2 Stratigraphic profiles of Pb concentration from (a) Bolivian and (b) Peruvian study sites. The uppermost samples dating to the 20 th century have been removed to highlight pre-industrial changes down-core.	47
Figure 3.3 Stratigraphic profiles of Pb flux from (a) Bolivian and (b) Peruvian study sites shown alongside (c) regional cultural chronology. The dashed line in (b) represents the division of the Late Intermediate Period (LIP) into the Wanka I and Wanka II cultural phases (see text). As in Figure 3.2, the uppermost samples dating to the 20 th century have been removed to highlight pre-industrial changes down-core.....	48
Figure 3.4 Prior to 500 AD at L. Taypi Chaka Kkota and 1000 AD at Lobato, the natural flux of Pb to each lake was stable and low representing pristine Pb accumulation levels. In addition, both Pb records are stable during pronounced periods of aridity as demonstrated by the lake level reconstruction for Lake Titicaca from Abbott <i>et al.</i> (1997a).	49

ACKNOWLEDGEMENTS

Various individuals contributed to the success of this project and it would not have been possible without their support and encouragement.

Professors Charlie Jones, Jim Richardson and Michael Rosenmeier always had time to talk over an idea (or simply listen) and I am grateful for their insight. Broxton Bird offered his friendship both in the field and in the office, and made both Pittsburgh and Peru much more enjoyable. In the lab, Brian Games and John Kittleson provided much needed chemistry tutoring, and Mark Abbott, always with an open door, challenged me and provided shape to my ideas.

Last but certainly not least, Tara not only moved to Pittsburgh with me, but has loved and supported me every step of the way.

Funding for this research was provided by the Committee for Research and Exploration of the National Geographic Society and by the University of Pittsburgh.

1.0 INTRODUCTION

1.1 PRE-COLONIAL METALLURGY IN THE ANDES

The Andes are the largest source of mineral wealth in the Americas and the origin of New World metallurgy. Metallurgical exploitation of these resources occurred for millennia prior to colonial contact, as is testified by numerous artifacts of gold, silver and bronze. Prior to the arrival of Spanish conquistadors in 1532 AD, indigenous South Americans smelted silver ores, hammered gold sheets, and annealed copper alloy sheets, independently of technologies that were by then highly developed in the Old World. Despite this extensive history, we know little about the development of metallurgical techniques through time.

Today we learn about ancient metallurgy primarily through three sources of information. The first is the collection and analysis of artifacts recovered from archaeological excavations. However, looting of archaeological sites is pervasive and as a result the archaeological record is incomplete (Jones and King, 2002). This means that archaeologists often work with either a small fraction of the original material or with artifacts that have been removed from their original context. Moreover, looters frequently “restore” looted artifacts, severely limiting what information can be drawn from their appearance (Shimada and Griffin, 2005). The second source of information comes from historical and ethnographical data collected at the time of conquest. For record keeping purposes, Spanish conquistadors documented the looting of Inca palaces and exploitation of Inca mines (Lechtman, 1976). Useful as these archives are, they tell

us little about those peoples who preceded the Inca. Moreover, the Spanish were primarily concerned with the acquisition of gold and to a lesser extent silver. They make little mention of copper and copper alloys, even though these represent the foundation of Andean metallurgy. The third method is that of archaeometry. Archaeometry is the application of scientific methods to archaeological sites or artifacts. In the Andes, the most common archaeometric analysis employed is a compositional chemical analysis (Lechtman and Klein, 1999; Lechtman, 2002). Recently, scientists have also utilized geochemical analysis of lake sediments to track atmospheric pollution from smelting (Abbott and Wolfe, 2003). This method provides an independent record of the timing and intensity of smelting for the region.

1.2 SMELTING IN THE ANDES

The most complete record of smelting technology comes from the *altiplano* of southern Bolivia. There, the Cerro Rico de Potosí silver deposit was once the world's richest silver mine. Given its richness, Potosí was the central focus of Colonial mining for years after conquest. As a result of this attention, a written chronicle exists of post-Colonial smelting techniques in use at Potosí. For example, between 1545 and 1572 AD, all silver production under colonial rule was conducted by Inca silversmiths using indigenous furnaces. Three different types of furnace were recorded by the Spanish during this time as they worked Potosí and the nearby mine of Porco. The first type of furnace was simply a pit dug into the ground that reduced ores rich in silver. The second type was a small, and sometimes portable, reduction furnace called a *huayara*. These charcoal-fired, wind-drafted furnaces were lined with clay and were often placed on mountain tops to take advantage of strong winds. As such, they were prone to destruction by any

number of natural forces (e.g. landslides, earthquakes). Recently, a *huayara* was found still in use today in Bolivia, and limited archaeological remains of an ancient *huayara* have also been recorded (Van Buren and Mills, 2005). The third type of furnace was a *tochochimpu*, which was normally used to refine silver in combination with argentiferous galena (lead sulphide) known as *soroche*. Cieza de León was one of the first Spanish chroniclers to describe the use of *soroche* at Potosí. He documented its use as a flux to enable extraction of silver from even low-grade ores. Future research combining historical archives, archaeological and ethnoarchaeological research should illuminate patterns of the spatial and temporal homogeneity of smelting technology in the southern Andes.

Despite these advances in tracing the smelting of ores, direct analysis of the metal artifacts themselves is the most common analytical approach. The most frequent investigation performed is that of a compositional analysis which determines the relative proportions of the metals which make up an artifact. This has shown that the vast majority of Andean artifacts are composed of alloys. Alloys, rather than pure metals, are pervasive in both Old and New World metallurgy for three reasons. First, occurrences of pure copper, silver and gold do not commonly occur in any large quantity. Second, alloys have the benefit of often being harder than objects made of native metal, as is the case with silver and gold (Lechtman, 1996). Third, by combining one or more metals, the melting temperature of those metals is lowered, which facilitates the smelting of ores. This is important as all pre-Columbian metallurgy was done without the use of bellows and had to rely on natural drafts to aerate furnaces.

The most common alloys found in southern South America have been those of arsenic-copper (arsenic bronze), tin-copper (tin bronze) and ternary alloys of copper, arsenic and nickel. There is also evidence that the Inca alloyed bismuth in bronzes recovered from the site of Machu

Picchu (Gordon and Rutledge, 1984; Gordon and Knopf, 2006). Alloys composed of copper-gold (a binary alloy sometimes referred to as *tumbaga*) and copper-silver-gold (a ternary alloy) have also been found, though not in the same quantity as copper alloys. The precious metal artifacts that are found normally occur as items of personal adornment (e.g. discs, bracelets, rings, and pendants) associated with individuals of high social status and as religious or ceremonial items (Olsen Bruhns, 1994). Because of the extensive looting that has taken place in Peru, both recently and during colonial times, few precious metals remain and our understanding of them remains comparatively sparse.

2.0 1500 YEARS OF METALLURGY RECORDED BY LAKE SEDIMENTS FROM THE CENTRAL PERUVIAN ANDES

2.1 INTRODUCTION

The South American Andes represent the largest source of mineral wealth in the Americas and the birthplace of New World metallurgy. Status among Andean peoples was imparted by what one wore both in life and death. In this regard, metal was second only to cloth in importance and was intimately associated with rank and power, influencing both secular and religious spheres of life (Lechtman, 1984). Despite a rich history of metallurgy subsequent to Hispanic conquest, little is known about the loci and intensities of earlier metallurgical activities. Natural processes, colonial mining following conquest, and modern industrial mining activities have destroyed most physical remains of early mining operations (Lechtman, 1976). Geochemical analyses of lake sediment records offer one strategy to infer early metallurgical activities (Renberg *et al.*, 1994; Abbott and Wolfe, 2003).

This study aims to complement the archaeological record of metallurgy from the central Peruvian Andes. Having been subject to four decades of extensive archaeological research, the pre-history of the central Peruvian Andes is well described (Earle *et al.*, 1980; D'Altroy and Hastorf, 1984; Costin *et al.*, 1989; Hastorf *et al.*, 1989). A large number of metal artifacts and metal production tools have been recovered during archaeological excavations. However, metal production findings are limited to the late stages of metal production. Ore acquisition and

smelting are thought to have occurred at the mining sites themselves (Howe and Petersen, 1992). Therefore, lake sediment records recovered near ancient mining centers should provide insights into ancient metallurgical activity.

Most studies of pollution involving natural archives focus on extra-regional to hemispheric-scale processes (e.g. Boutron *et al.*, 1991; Renberg *et al.*, 1994; Rosman *et al.*, 1994; Renberg *et al.*, 2002). While a few studies have been directed towards regional-scale reconstructions (Monna *et al.*, 2004; Baron *et al.*, 2005; Donahue *et al.*, 2006; Gallon *et al.*, 2006), only two studies have examined metal and metalloid burdens in Andean lake sediments (Espí *et al.*, 1997; Abbott and Wolfe, 2003). Lead (Pb) is commonly used as the cornerstone for metallurgical reconstructions because it is not appreciably affected by post-depositional mobility (Renberg *et al.*, 2002; Gallon *et al.*, 2004). In addition, Pb isotopic ratios exhibit natural variability that can trace ore provenance (Dickin, 1995). The Pb isotopic ratio of ore minerals (e.g. lead sulfides such as galena) does not evolve after formation given the small amounts of parent uranium (U) or thorium (Th) isotopes. Lead isotopic ratios are not fractionated after deposition in natural media including lake sediments. As a result, Pb isotopic ratios are sensitive indicators of pre-industrial pollution and ore provenance (Sangster *et al.*, 2000; Renberg *et al.*, 2002). Lead is especially useful in the Andes because galena (locally known as *soroche* meaning “that which makes run or slip”) was used as a flux during smelting of silver (Ag) bearing ores (Bakewell, 1984). Here, we combine Pb concentrations and isotopic ratios with a suite of additional elemental concentrations and demonstrate that paleolimnology provides a novel approach for addressing archaeometallurgical questions.

2.2 STUDY SITES

The Andes mountains extend nearly 7,500 km along the west coast of South America. The city of Cerro de Pasco is located on the *altiplano* (high plateau) of central Peru (Figure 2.1). The central Andes host numerous polymetallic Cu-Pb-Zn-Ag orebodies. Of these, the massive oxidized zones (*pacos*) were the first to be exploited (Purser, 1971). With an elevation of 4380 m, Cerro de Pasco is the highest city of its size (>20,000 people) in the world. After its discovery by the Spanish in 1630 AD, the region became one of the world's foremost producers of silver (Fisher, 1977). The orebodies at Cerro de Pasco are associated with Tertiary volcanic vents located in the core of a non-plunging anticline of Devonian age (Ward, 1961). In addition to native silver, the principal ores contain combinations of arsenopyrite (FeAsS), aramayoite [Ag(Sb, Bi)S₂], chalcopyrite (CuFeS₂), enargite (Cu₃AsS₄), argentiferous galena [(Ag, Pb)S], tennantite (Cu₁₂As₄S₁₃), grantonite (Pb₉As₄S₁₅), and sphalerite [(Zn, Fe)S] (Ward, 1961; Einaudi, 1977). Today, Cerro de Pasco is an open pit mine, noted more for copper production, but also for gold, lead, bismuth, and zinc (Benavides Q., 1990). The mine is estimated to have contained one-thousand tons of silver, four million tons of zinc, two million tons of lead, and lesser amounts of gold and bismuth prior to Colonial exploitation (Peterson, 1965a; Einaudi, 1977).

Laguna Chipian (10° 43' S, 76° 10' W) rests on carbonate terrain of Jurassic age ~9 km southeast of Cerro de Pasco (Figure 2.2). Laguna Chipian (Figure 2.3a, b) is a small (0.12 km²), shallow (3 m), alkaline (pH=10) lake occupying a catchment of 2.81 km². Surface winds can be quite variable, but are predominantly from the west. A large collection of Colonial smelters and grinding wheels (locally called *batans*) (Figure 2.3c, d) are located in the valley bottom below Laguna Chipian. Also located very near to the smelters are a number of small excavations believed to be Colonial pit mines.

The Morococha mining region is located in the Junin district of the western Cordillera. Morococha is situated over replacement bodies, such as mantos, chimneys and skarns (Gunneshch *et al.*, 1990). In addition to native silver, the richest ores at Morococha contain combinations of anhydrite (CaSO_4), barite (BaSO_4), bourmonite (CuPbSbS_3), arsenopyrite, chalcopyrite, emplectite (CuBiS_2), enargite, galena, matildite (AgBiS_2), proustite ($\text{Ag}_3\text{As}_3\text{S}_3$), sphalerite, stromeyerite (AgCuS), and tennantite (Ward, 1961; Einaudi, 1977). Morococha was reportedly discovered during the 17th century by Colonial metallurgists (Purser, 1971).

Located 11 km northeast of modern silver mining operations at Morococha (Figure 2.4a), Laguna Pirhuacocha ($11^\circ 31' \text{ S}$, $76^\circ 04' \text{ W}$) occupies Cretaceous carbonate terrain. The lake is circumneutral and is 18 m deep. The lake is small (0.05 km^2) and occupies a non-glacial catchment of 3.14 km^2 . Laguna Pirhuacocha drains to the east during the wet season (December to March) through a small creek, and a small littoral bench sits at the mouth of this creek (Figure 2.4b). Surface winds driven by daytime heating blow predominantly from the west rising up the valleys and sinking back down the valleys at night.

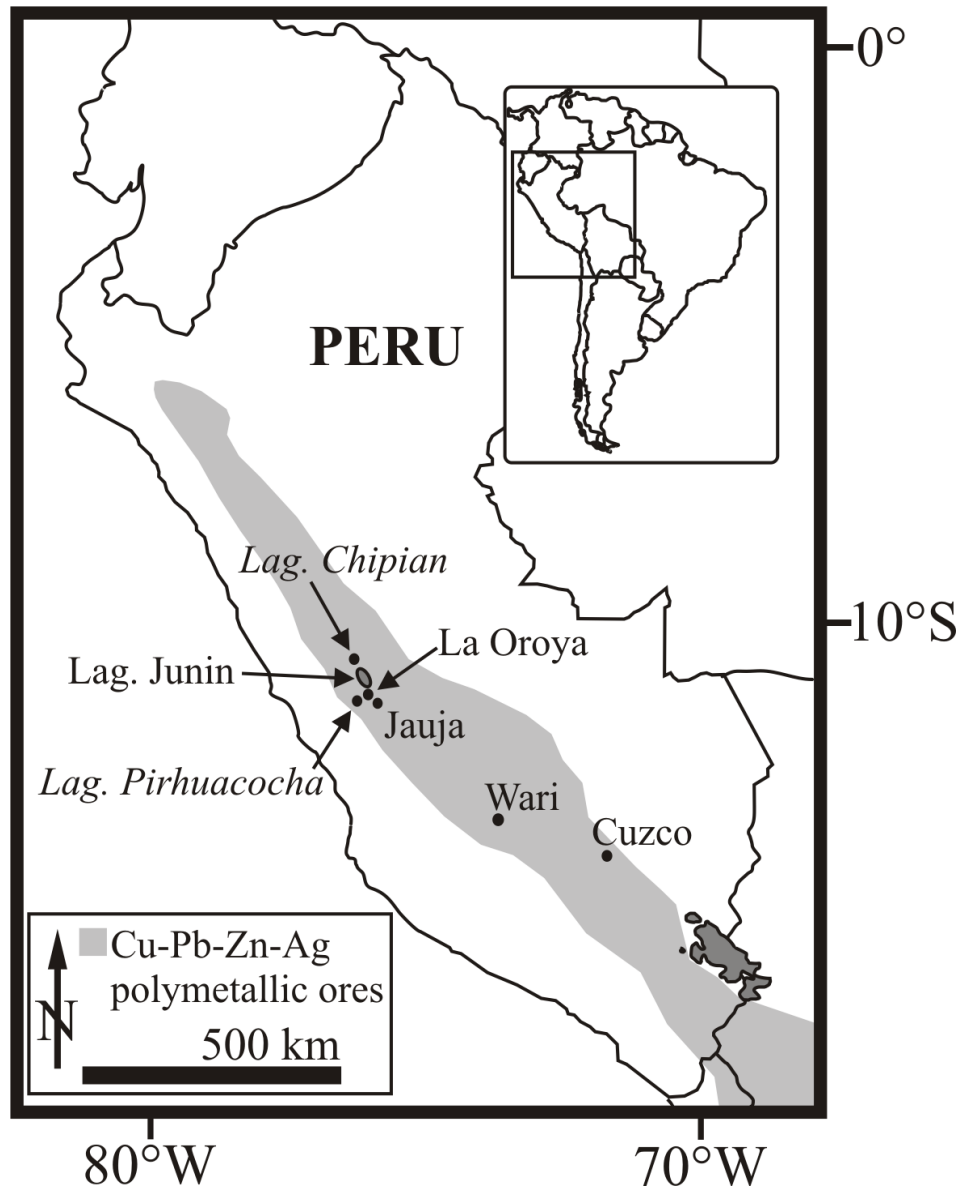


Figure 2.1 Map of Peru showing lake study sites (*italics*), archaeological sites and towns discussed in text.

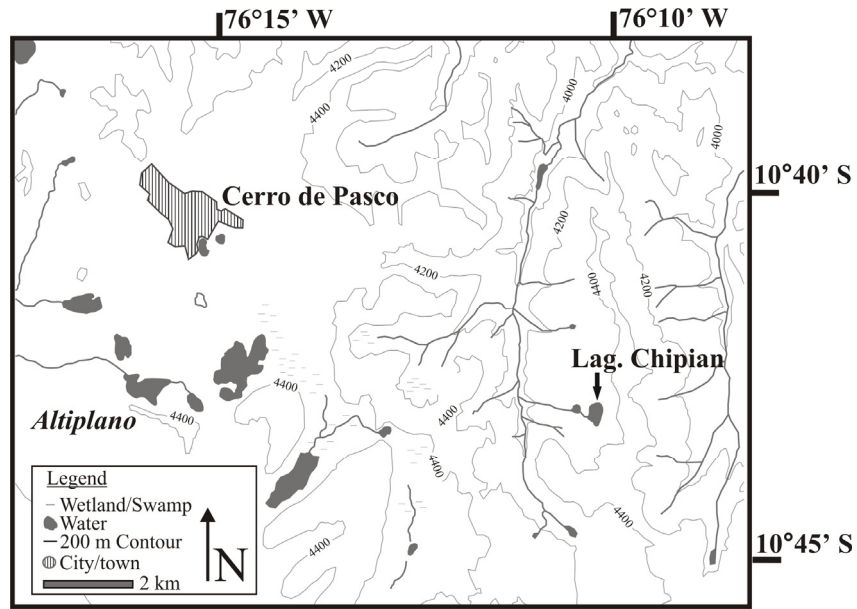


Figure 2.2 Base map of Laguna Chipian and the Cerro de Pasco area.

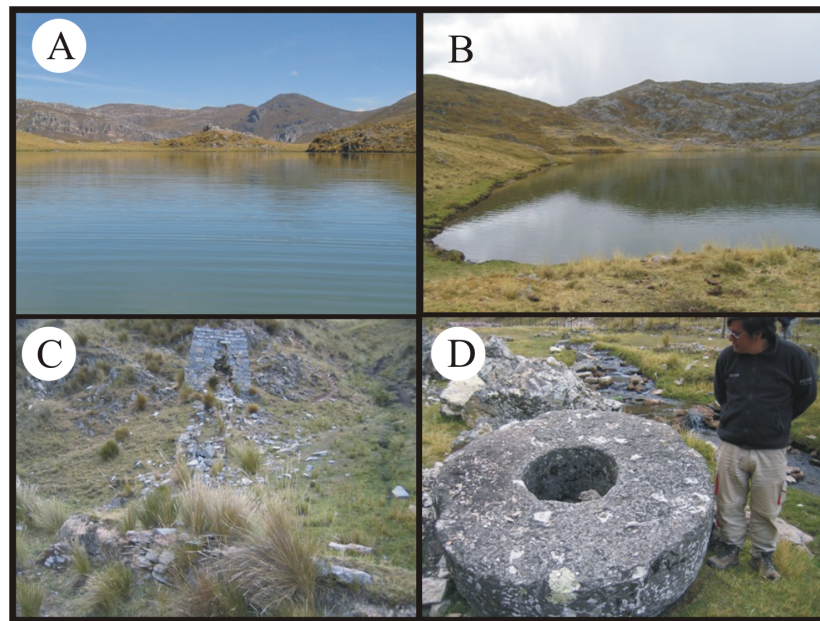


Figure 2.3 Photos of Laguna Chipian (a and b), a presumed smelter and patio (c) and a large grinding wheel (d). The smelter and grinding wheel are located within the valley below the lake and are presumed to be colonial in age.

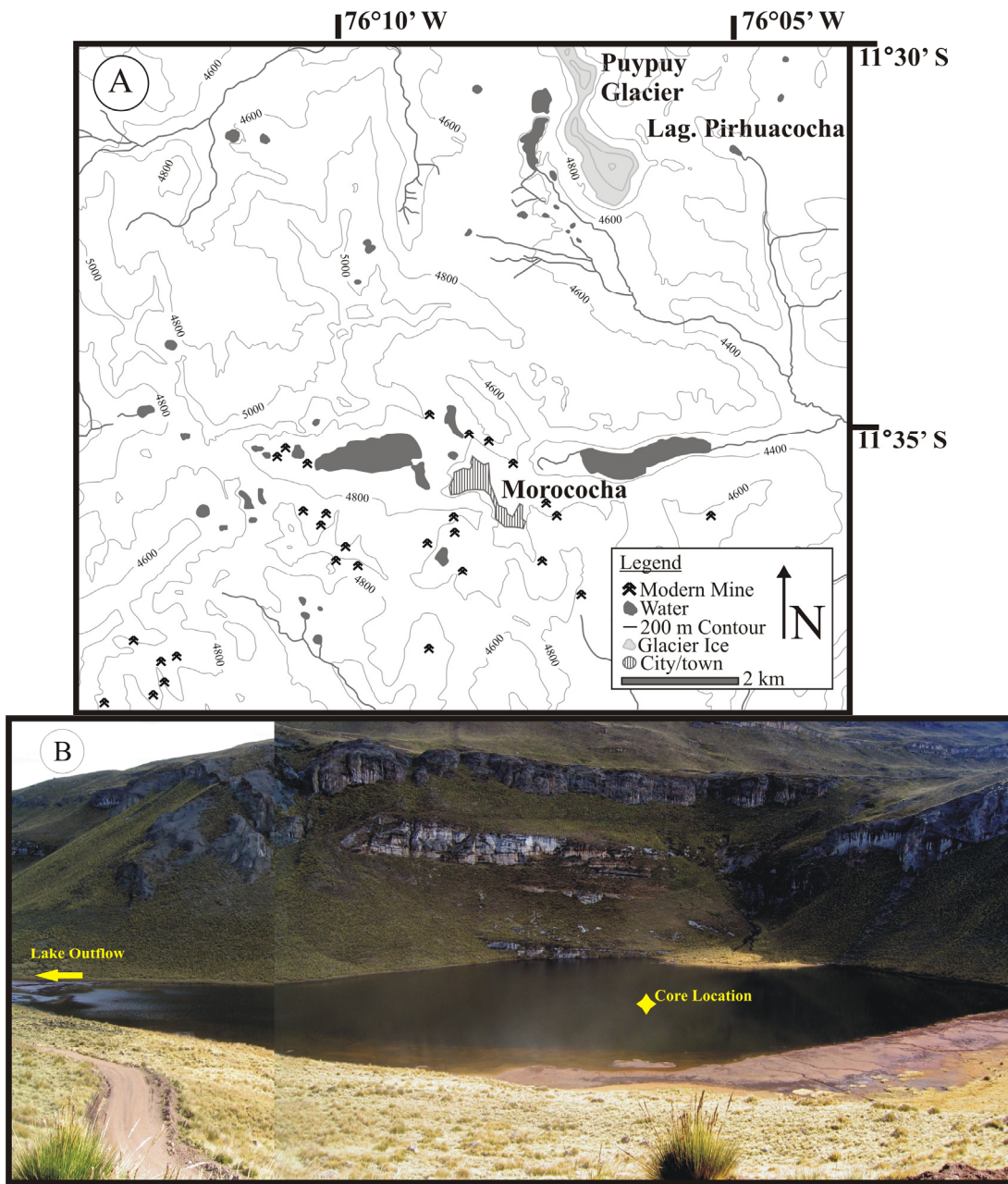


Figure 2.4 (a) Base map of Laguna Pirhuacocha and the Morococha mining area. (b) Photo looking west-southwest showing coring location and the direction of outflow.

Basic limnological characteristics for both lakes are summarized in Table 2.1. Located well away from all modern day mining activities, the study sites are ideally suited to record atmospheric fallout of smelting emissions, both past and present.

Table 2.1 Limnological parameters for the study lakes.

Sample	Temp °C	D.O. mg L ⁻¹	Conductivity mS cm ⁻¹	pH
Pirhuacocha epilimnion	10.58	5.68	0.2686	7.83
Pirhuacocha hypolimnion	8.20	5.34	0.2714	7.81
Chipian epilimnion	11.65	9.4	0.1623	10.66
Chipian hypolimnion	10.875	9.84	0.157	10.66

2.3 METHODS

2.3.1 Core collection and chronology

During May and June of 2005, sediment cores were collected from the deepest points of Lagunas Chipian and Pirhuacocha using a slide hammer corer fitted with a 7-cm diameter polycarbonate tube (Blomqvist, 1991). Both cores contained an intact sediment-water interface, with no visible disturbance to the sediment column. The entire 62 cm core from Laguna Chipian and the upper 15-cm of the Laguna Pirhuacocha core were extruded in the field into continuous 0.5-cm increments to eliminate potential disturbance. The upper sediments of each core were dated using ²¹⁰Pb activities ($t_{1/2} = 22.3$ years), measured by α -spectroscopy in order to construct an age-depth model for recent sedimentation. To constrain changes below the limit of ²¹⁰Pb

methodology (100 to 150 years), two radiocarbon dates from Laguna Chipian and six from Laguna Pirhuacocha were obtained from aquatic macrophytes and charcoal.

2.3.2 Geochemical characterization

Elements were extracted from both cores using dilute acid extraction techniques. At Laguna Chipian, every 2-cm was sampled and analyzed, while at Laguna Pirhuacocha every 0.5-cm from 0 to 60 cm and every 2.5-cm from 60 to 87.5 cm were sampled. All samples were freeze-dried and homogenized. Digestion and dilution vessels were acid cleaned and triple rinsed using 18 M Ω ultrapure water. Between 0.1 (Laguna Chipian) to 0.5 g (Laguna Pirhuacocha) of precisely weighed sediment was extracted using 10 ml of 1.6 M Optima grade HNO₃ at room temperature for 24 hours. Subsequent 1 ml aliquots of supernatant were then diluted to 10 ml using 2% Optima grade HNO₃.

This weak extraction procedure targets weakly-bound elements adsorbed to organic and inorganic surfaces and not those elements hosted in the lattice sites of detrital silicate minerals (Shirahata *et al.*, 1980; Ng and Patterson, 1982; Hamelin *et al.*, 1990; Kober *et al.*, 1999). Graney *et al.* (1995) reported that the strength and type of acid (e.g. HNO₃ vs. HCl) has little impact on either the concentration of the Pb leached or its isotopic signature. Furthermore, Graney *et al.* (1995) showed that the weakly-bound Pb is isotopically distinct from that contained within mineral lattices after total digestion with HF. This extraction therefore, contains most, if not all, of the anthropogenic input to the sediment.

A suite of elements were considered in order to constrain and interpret natural and anthropogenic geochemical changes. At Laguna Chipian, Pb and sulfur (S) were determined by inductively coupled plasma-atomic emission spectrometry (ICP-AES Spectroflame-EOP) at the

University of Pittsburgh, while arsenic (As), silver (Ag), copper (Cu), bismuth (Bi), and titanium (Ti) were measured using a Finnigan MAT double focusing magnetic sector ICP-Mass Spectrometer (ICP-MS ELEMENT) at Penn State University. From Laguna Pirhuacocha Cu, Pb, S, and Ti were determined using ICP-AES while Ag, As, and Bi were quantified on the ICP-MS. The elements analyzed by each instrument and the associated instrument detection limits (IDL) are shown in table 2.2. Concentrations were verified against the certified multi-element standard, SPEX ICP-MS-2. Analytical error was <10 % for every element run. Duplicates were run every 10th sample and were constantly within 8 % of each other. A minimum of 6 blanks or 10 % the number of samples (whichever was greater) was carried through the entire procedure with each batch of samples (Boyle, 2001). Blanks were consistently below IDL for each element. All elemental concentrations are reported as $\mu\text{g g}^{-1}$ dry sediment mass unless noted.

Table 2.2 Instrument detection limits (IDL) and analytical error (1σ) for all elements measured from study sites. IDL and 1σ error are reported as $\mu\text{g g}^{-1}$ dry sediment mass.

		Chipian			Pirhuacocha				
		Element	IDL	$\pm (1\sigma)$	Element	IDL	$\pm (1\sigma)$		
ICP-AES	K	39	9		K	20.0	0.7	ICP-AES	
	Mn	6	1		Mn	2.4	0.1		
	Zn	2.6	0.6		Zn	0.7	0.1		
	Al	92	20		Al	47	6		
	S	46	10		S	24	3		
	Na	28	6		Na	14	1		
	Fe	23	5		Fe	11	1		
	Pb	54	2		Pb	4.8	0.6		
	Ni	3.0	0.6		Ni	9	1		
ICP-MS					Ti	2.2	0.3	ICP-MS	
					Co	1.5	0.2		
	Ag	0.003	0.001		Cu	5.4	0.7		
	Cd	0.004	0.001		V	5.0	0.6		
	Sn	0.003	0.001						
	Sb	0.0009	0.0002		Ag	0.00023	0.00003		
	Bi	0.0003	0.0001		Cd	0.0010	0.0001		
	Ti	0.07	0.01		Sn	0.00049	0.00006		
	V	0.020	0.004		Sb	0.00009	0.00001		
	Co	0.011	0.002		Bi	0.00009	0.00001		
	Cu	0.06	0.01		As	0.019	0.002		
	As	0.12	0.03						

2.3.3 Lead isotopes

Lead isotopic ratios were measured by ICP-MS. All isotope ratios were calculated after blank subtraction, and mass-bias corrections were made using NIST SRM 981 (common Pb isotopic standard). Instrument parameters were based on Townsend and Snape (2002). The relative standard deviation (RSD) was less than 0.3% for all Pb isotopic measurements.

2.4 RESULTS

2.4.1 Core chronology

2.4.1.1 Laguna Chipian

Laguna Chipian sediment was tan, massive, and predominantly composed of carbonate material. The sediment was apparently well oxidized with no visible redox front below the sediment-water interface.

Total ^{210}Pb activity at Laguna Chipian displays a conspicuous non-monotonic behavior in the uppermost 8 cm superimposed on an otherwise exponential decline down-core (Figure 2.5a). Unsupported ^{210}Pb activity was calculated by subtraction of the estimated supported activity (determined by averaging the activity of the lowermost four samples in the core) from each sample (Binford, 1990). The non-monotonic behavior of ^{210}Pb observed in the uppermost sediment implies that either sedimentation rates have increased during the 20th century, effectively diluting the ^{210}Pb inventory, or that sediment mixing has occurred in the uppermost sediment. Laguna Chipian is a shallow lake (3 m) and the homogeneous $^{206}\text{Pb}/^{207}\text{Pb}$ profile observed within the uppermost 8 cm (see results below) would suggest physical mixing is the cause of the flattening of ^{210}Pb activity. This sediment mixing does not appear to have appreciably affected sediment deeper in the core, as $^{206}\text{Pb}/^{207}\text{Pb}$ and elemental concentrations are highly variable down-core. A mixed surface layer is permissible in the constant rate of supply (CRS) dating model (Bindler *et al.*, 2001), thereby allowing for the construction of an age-depth relationship profile.

To obtain sediment ages beyond the limit of ^{210}Pb dating, accelerator mass spectrometer (AMS) ^{14}C dates were obtained on charcoal. Radiocarbon dates are shown in table 2.3 and

Figure 2.5a. All dates reported here were converted to calendar years AD using the calibration program Calib 5.0 (Reimer *et al.*, 2004). Linear interpretation between ^{14}C dates and the base of the ^{210}Pb chronology provides a composite chronological model (Figure 2.5a).

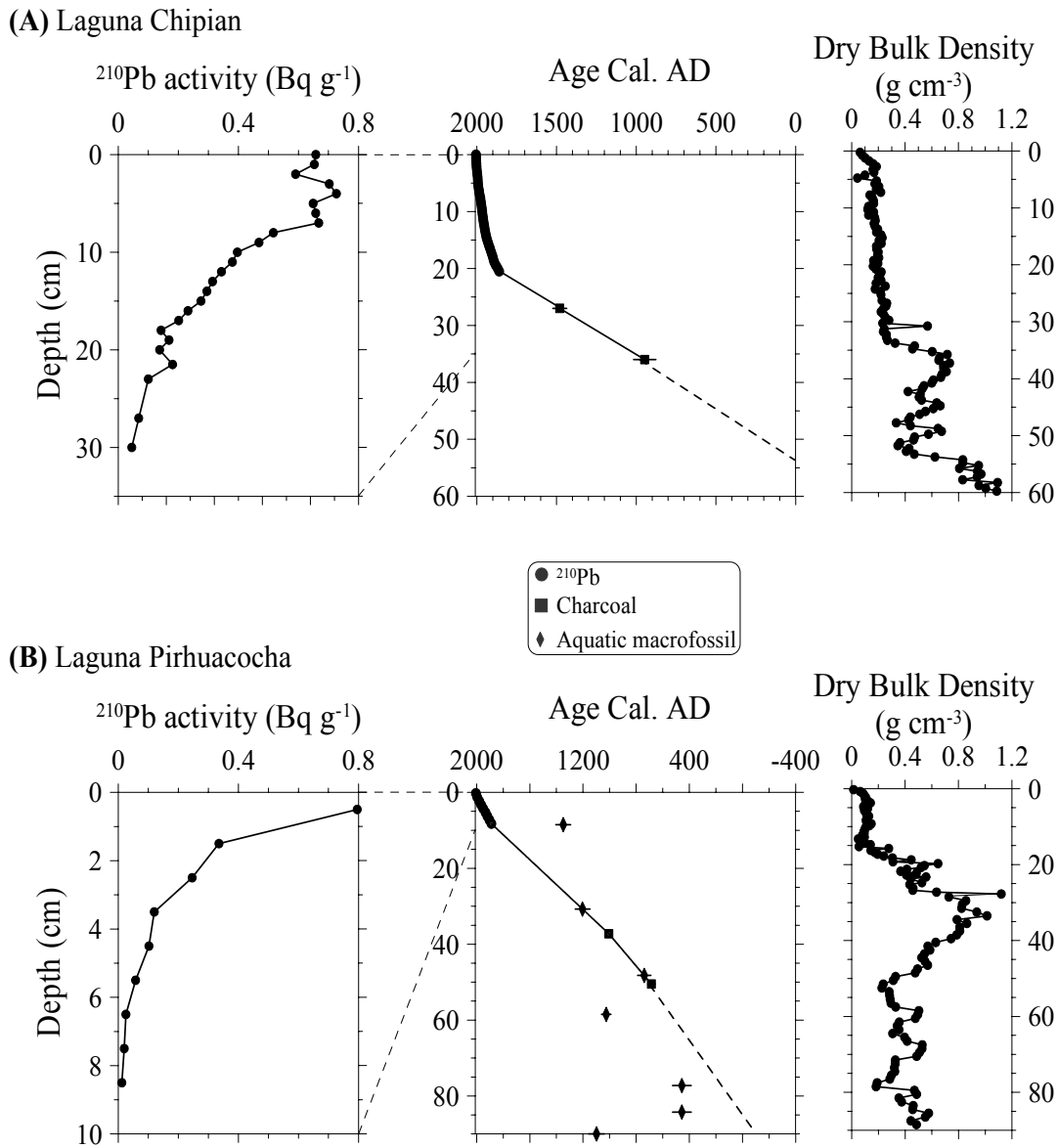


Figure 2.5 Down-core sediment ^{210}Pb activities, composite age-depth models and bulk density profiles for (a) Laguna Chipian and (b) Laguna Pirhuacocha. Only those dates obtained on charcoal were used to construct age-depth models (see text). Error bars represent the 2σ error range on dates; error bars not shown are smaller than the data points displayed.

2.4.1.2 Laguna Pirhuacocha

The Laguna Pirhuacocha core experienced some compaction and water loss in the uppermost ~5 cm of the core (core depth 15 to 20 cm) during shipment back to the University of Pittsburgh. The Laguna Pirhuacocha sediment was massive, organic rich, olive-brown gyttja and contained no visible stratigraphy. In addition, the core was apparently well oxidized at its surface, with no abrupt redox front below the sediment-water interface.

^{210}Pb activity declines monotonically from a surface value of 0.80 Bq g^{-1} to a relatively steady supported background of 0.03 Bq g^{-1} at depths below 8.5 cm (Figure 2.5b). The constant initial concentration (CIC) model was applied to calculate sediment ages because sediment accumulation rates are near-constant ($0.007 \pm 0.0003 \text{ g cm}^{-2} \text{ yr}^{-1}$) (Appleby, 2001). Dating uncertainty based on this model is less than ± 5 years for the period of record.

Accelerator mass spectrometry (AMS) ^{14}C dates were obtained on charcoal and aquatic plant macrofossils. The aquatic (and possibly rooted) macrophytes initially selected for absolute dating proved unreliable recorders of atmospheric ^{14}C . For example, at the 8 to 8.5 cm interval, the ^{210}Pb calculated age is 1888 AD ± 25 years. However, an aquatic macrophyte from the same interval yielded a ^{14}C derived date of 1348 AD ± 60 years. This suggests a hard-water reservoir effect of ~600 years. A reversal was also noted, and different sediment intervals yielded identical dates (at 77 and 84 cm) (Figure 2.54b, Table 2.2). Thus, the age-depth model for Laguna Pirhuacocha relies entirely on the charcoal dates. As with Laguna Chipian, linear interpolation between ^{14}C dates and the base of the ^{210}Pb chronology provides for a composite chronological model (Figure 2.5b).

2.4.2 Core geochemistry

2.4.2.1 Laguna Chipian

At Laguna Chipian, a coarse sampling interval and a slow sedimentation rate yield centennial-scale resolution. All elemental profiles shown in Figure 2.6 are plotted against core depth. Titanium remains relatively flat throughout the entire length of the sediment record with a single spike in the upper 10 cm of the core. A peak in S around 30 cm marks the divide between low S below and high S above. The first evidence for enrichment of metallurgical elements at Laguna Chipian also occurs ~30 cm depth as As, Bi, Cu, and Pb increase during this interval (Figure 2.6). Based on the age model, this increase occurs sometime between 1000 and 1270 AD. All four metals display a gradually increasing trend until ~22 cm, after which they rapidly increase to a peak at ~7 cm depth. This rapid increase in metal concentration starts at ca. 1860 ± 40 AD and peaks at 1917 ± 13 AD based on the ²¹⁰Pb chronology. Metal concentrations subsequently decline up-core. Silver represents an exception to this trend, remaining flat along the entire length of the core with the exception of a single datum dated to the early 1990s.

Laguna Chipian

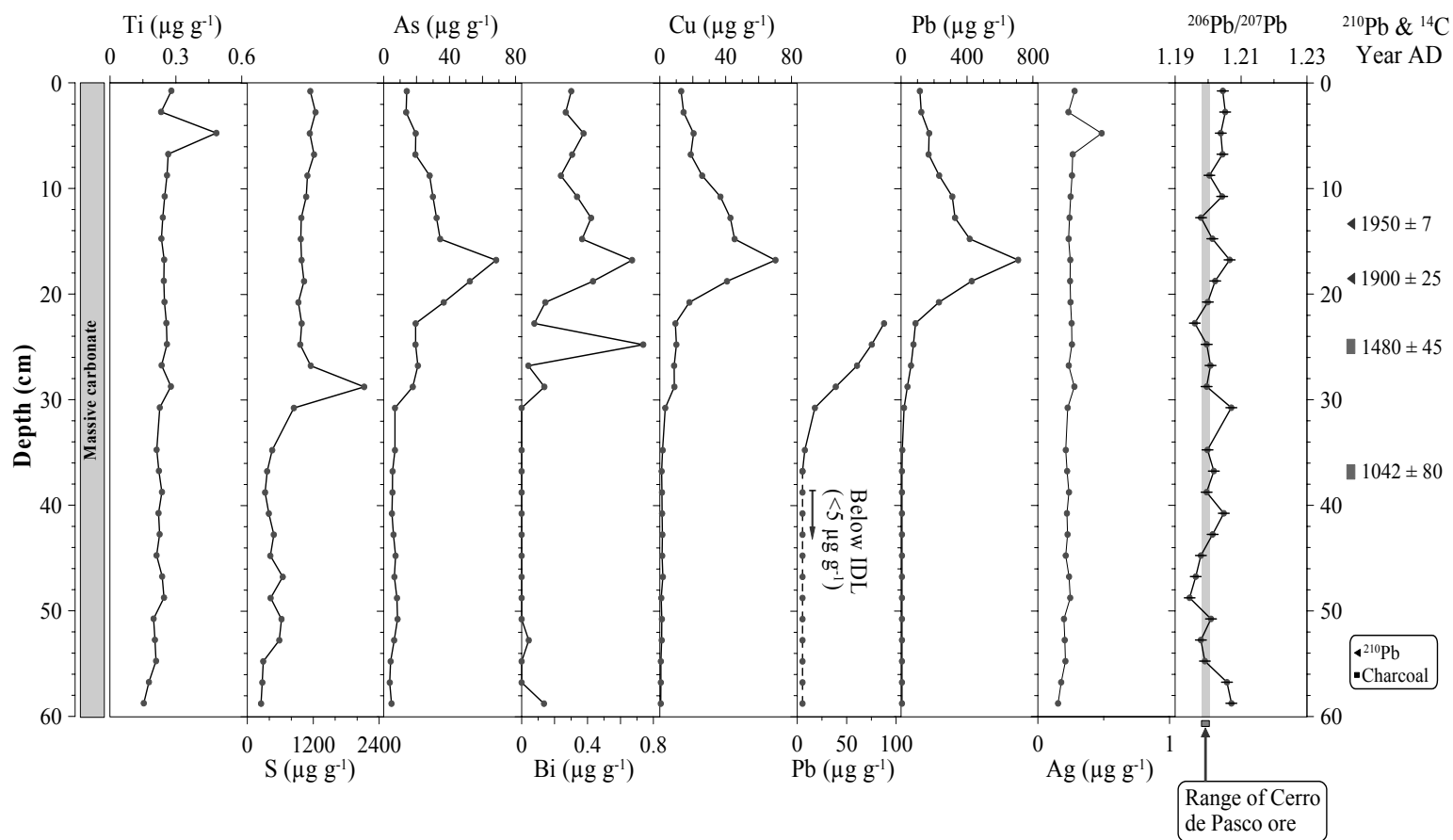


Figure 2.6 Geochemical and isotopic stratigraphies and associated ^{210}Pb and ^{14}C dates for Laguna Chipian. All elemental concentrations are reported as $\mu\text{g g}^{-1}$ dry sediment mass. Analytical error bars are smaller than the data points shown. Two separate plots of Pb are shown to highlight smaller enrichments deeper in the core. Published $^{206}\text{Pb}/^{207}\text{Pb}$ isotopic ratios of Cerro de Pasco ore from Mukasa *et al.* (1990) and Sangster *et al.* (2000).

2.4.2.2 Laguna Pirhuacocha

The uppermost 5 cm of the Laguna Pirhuacocha core (dating to the 20th century) are characterized by extremely high values for many of the elements examined. Therefore, they have been largely omitted from Figure 2.7 and are presented separately in Figure 2.8. Titanium fluctuates between 25 and 100 $\mu\text{g g}^{-1}$ along the entire length of the core, with a notable peak between 10 and 15 cm. Sulfur and As are coupled ($r^2=0.72$; $n=127$; $P<0.001$) until the upper 5 cm, suggesting that sulfides were the primary sequestration mechanism for sedimentary As. Both S and As also display a peak at 10 to 15 cm (ca. 1700 to 1850 AD); after this point the two profiles become decoupled ($r^2=0.27$; $n=10$; $P=0.17$). While S fluctuates before declining rapidly in the uppermost 1.5 cm of sediment, As steadily increases towards the core top, eventually reaching $\sim 1100 \mu\text{g g}^{-1}$ at the sediment-water interface (Figure 2.8). Below 5 cm depth, As retention appears to have been S limited while the decoupling of As and S in the uppermost sediments is likely due to enhanced rates of As deposition relative to S.

Bismuth remains near the IDL until ~ 30 cm (ca. 1200 AD), after which point it increases in tandem with As except for a subsurface peak of $\sim 80 \mu\text{g g}^{-1}$ at 3 cm (1975 AD; Figure 2.8). The Cu and Ag profiles increase earlier than the other metals at 60 cm (ca. 500 AD), though Cu displays considerably more background variability below 60 cm than Ag. Copper also peaks around 40 cm then declines until the last 5 cm of the core, after which it reaches $160 \mu\text{g g}^{-1}$ by 1975. Within the Ag profile are two large increases at 50 and 41 cm, which obscure smaller fluctuations along the length of the core. Therefore, another plot of Ag is shown with these points and the upper 5 cm removed.

Two plots of Pb concentration are shown to highlight smaller fluctuations down-core. Lead displays a gradual increase beginning around 60 cm, but does not exceed background

variability established between ~50 and 90 cm until 45 cm. A clear increase in Pb concentration occurs by 30 cm (1200 AD). Above 20 cm, Pb increases dramatically, rising to 100 and 160 $\mu\text{g g}^{-1}$ by the early 20th century. Lead concentrations subsequently increase to over 2700 $\mu\text{g g}^{-1}$ by 1975 AD only to decline to ~1500 $\mu\text{g g}^{-1}$ at the sediment-water interface.

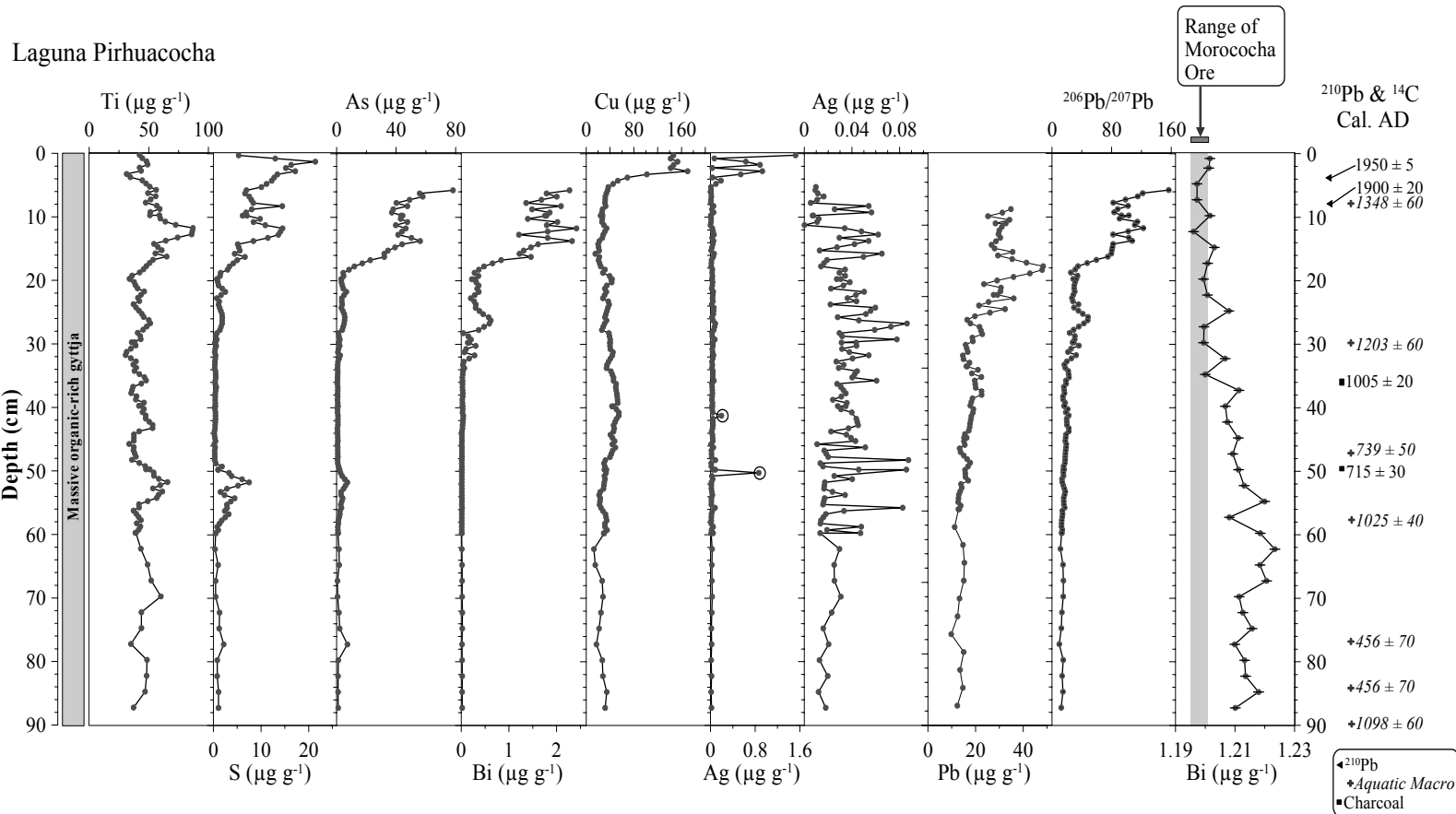


Figure 2.7 Geochemical and isotopic stratigraphies and associated ^{210}Pb and ^{14}C dates for Laguna Pirhuacocha. Note the two separate plots of Ag, with the second plot omitting circled data points and top 5 cm. Also note the two plots for Pb using different scales, and the omission of the top 5 cm of data for Pb, Ag, Cu, Bi, and As in order to highlight trends down-core. The omitted data are shown separately in Figure 2.8. All elemental concentrations are reported as $\mu\text{g g}^{-1}$ dry sediment except for S, which is in mg g^{-1} .

Published $^{206}\text{Pb}/^{207}\text{Pb}$ isotopic ratios of Cerro de Pasco ore from Gunnesch *et al.* (1990) and Macfarlane *et al.* (1990).

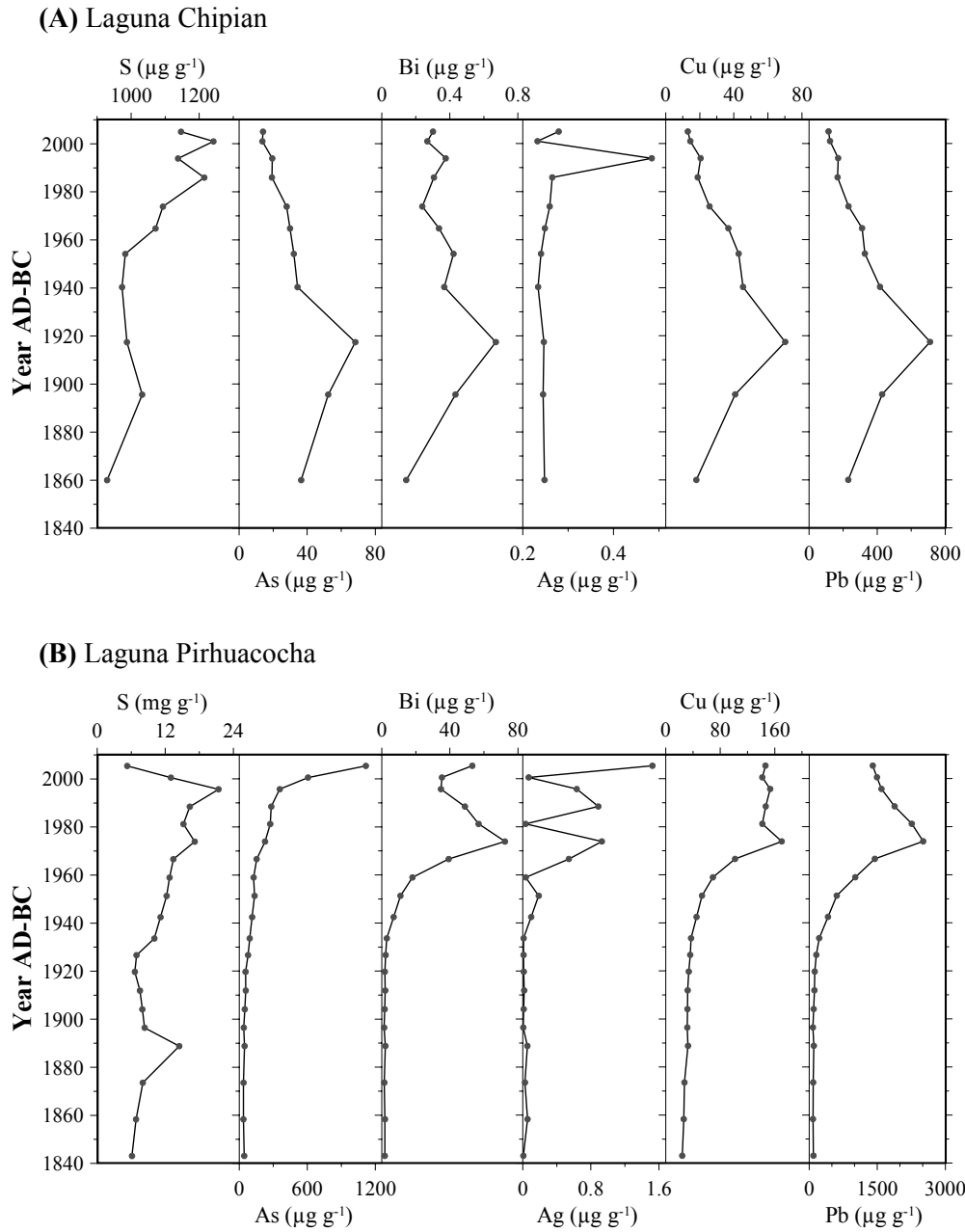


Figure 2.8 Industrial era geochemical histories for the last 150 years from (a) Laguna Chipian and (b) Laguna Pirhuacocha plotted against the ^{210}Pb chronologies.

2.4.3 Data preparation

Although concentration data are commonly used to interpret sediment geochemical records, such data must be considered with care. Concentrations may be enhanced or diluted by variations in mineral matter or major elemental fluxes (Norton and Kahl, 1991) or by changes in compaction or primary production (Outridge *et al.*, 2005). Both cores have experienced compaction as well as variable sedimentation rates through time (Figure 2.5). Thus, concentration data may not reflect actual rates of deposition through time. To correct for these biases, mass accumulation rate (i.e. flux) was calculated using the equation:

$$\text{Flux} = R_m \cdot \text{Metal}_{\text{conc}}$$

where: R_m is the sedimentation rate ($\text{g cm}^{-2} \text{yr}^{-1}$) and $\text{Metal}_{\text{conc}}$ is the elemental concentration in $\mu\text{g g}^{-1}$.

2.4.4 Isotopic contribution

Sediment Pb is isotopically impacted by even small increases in pollution Pb if isotopically distinct from background Pb. Therefore, Pb isotopic signatures can be used to infer anthropogenic activity when concentration data alone may be ambiguous (Renberg *et al.*, 2002; Townsend and Snape, 2002). To isotopically characterize pollution Pb, a measurable difference must exist between the isotopic ratio of natural or background Pb and the excess or pollution Pb. This is not a problem when assessing long range transport of pollutants, as ore isotopic ratios are regionally distinct (Sangster *et al.*, 2000); however, when assessing lake records that are located

proximal to or within a few kilometers of mining operations, natural and anthropogenic Pb may be isotopically indistinguishable.

2.4.4.1 Laguna Chipian

$^{206}\text{Pb}/^{207}\text{Pb}$ ratios at Laguna Chipian exhibit considerable homogeneity along the length of the core (Figure 2.6). Published ore $^{206}\text{Pb}/^{207}\text{Pb}$ variability for Cerro de Pasco falls within a relatively limited range (1.1985 to 1.2009; $n=4$) (Mukasa *et al.*, 1990; Sangster *et al.*, 2000) that overlaps with many of the sample isotopic ratios. The homogeneity of the $^{206}\text{Pb}/^{207}\text{Pb}$ profile may be due to both background and pollution Pb being derived from the same source (or multiple sources with the same isotopic ratio) or the post-depositional movement of Pb through the sediment column. Laguna Chipian is located in a small up-land depression. The valley below funnels surface winds blowing in from the west off the *altiplano*. Thus, background Pb may be derived from some of the same sources as the Pb ores targeted for mining. This would result in a static isotopic profile. The observed profile does not appear to have resulted from vertical migration of sediment Pb, as the Pb profile does not resemble that of known redox-sensitive elements (e.g. S, Fe and Mn). Furthermore, Pb concentrations are stable and low ($<5 \mu\text{g g}^{-1}$) for a millennium prior to enrichment and are characterized by a small but measurable differences in $^{206}\text{Pb}/^{207}\text{Pb}$. Any vertical migration of sediment Pb would result in a leveling of the Pb profile and the homogenization of the $^{206}\text{Pb}/^{207}\text{Pb}$ signature, as is observed in the core top. In addition, the observed peak in Pb concentration ($800 \mu\text{g g}^{-1}$) exceeds any published range of natural Pb variability in lake sediments by almost two orders of magnitude. Since no known natural processes can induce this level of enrichment, an anthropogenic source for the Pb must be considered.

2.4.4.2 Laguna Pirhuacocha

At Laguna Pirhuacocha, background $^{206}\text{Pb}/^{207}\text{Pb}$ is characterized by an increasing trend from the base of the core to 60 cm, above which it decreases (Figure 2.7). This decreasing trend continues into the modern era and stabilizes ~ 1.20 , a ratio consistent with published $^{206}\text{Pb}/^{207}\text{Pb}$ ratios for Morococha ore bodies (Gunnesch *et al.*, 1990; Macfarlane *et al.*, 1990). Thus, the uppermost sediments, which are characterized by extremely high Pb concentrations (Figure 2.8), are correlated with the lowest isotopic ratios (Figure 2.7). This declining trend in $^{206}\text{Pb}/^{207}\text{Pb}$ supports our contention that pollution Pb at Laguna Pirhuacocha is characterized by either a unique anthropogenic source (i.e. Morococha ore) or multiple sources with the same isotopic ratio. The relatively variable background $^{206}\text{Pb}/^{207}\text{Pb}$ ratio is likely caused by the high isotopic variation exhibited by local bedrock ($n=4$) (Gunnesch *et al.*, 1990). It also suggests that background Pb is delivered to the lake by atmospheric transport from the east, as $^{206}\text{Pb}/^{207}\text{Pb}$ ratios generally increase west to east in the Andes (Macfarlane *et al.*, 1990).

2.5 DISCUSSION

2.5.1 Pre-Colonial and Colonial metal pollution

Elemental concentrations and fluxes at Laguna Pirhuacocha are low prior to 700 AD. These represent natural background metal accumulation levels (Figures 2.7 and 2.9). Around 700 AD, Ag concentrations and fluxes both increase and become highly variable. At the same time, Cu reverses a declining trend, abruptly increasing, while $^{206}\text{Pb}/^{207}\text{Pb}$ begins to decline, dropping below background variability by 600 AD. Together, these three records represent the earliest evidence for atmospheric pollution within Laguna Pirhuacocha sediments. After this

initial pulse of metals, Cu and Ag both briefly decline, and $^{206}\text{Pb}/^{207}\text{Pb}$ rises to within background variability. However, this decline is short lived. By 750 AD, Cu increased two-fold and Pb enrichment becomes apparent. It is also after 750 AD that $^{206}\text{Pb}/^{207}\text{Pb}$ remains consistently below background variability. By 1000 AD, Cu flux exceeded $1.2 \mu\text{g cm}^{-2} \text{ yr}^{-1}$, an enrichment level not seen again until the 20th century. This, in combination with the previously described inverse relationship with $^{206}\text{Pb}/^{207}\text{Pb}$ (high Cu = low $^{206}\text{Pb}/^{207}\text{Pb}$), suggests that early metallurgy at Morocochoa was aimed at copper and copper alloys. The low Pb pollution during this period likely reflects lead's lack of involvement in the copper smelting process. Lead would have been released when ores containing it were unintentionally included in the furnace.

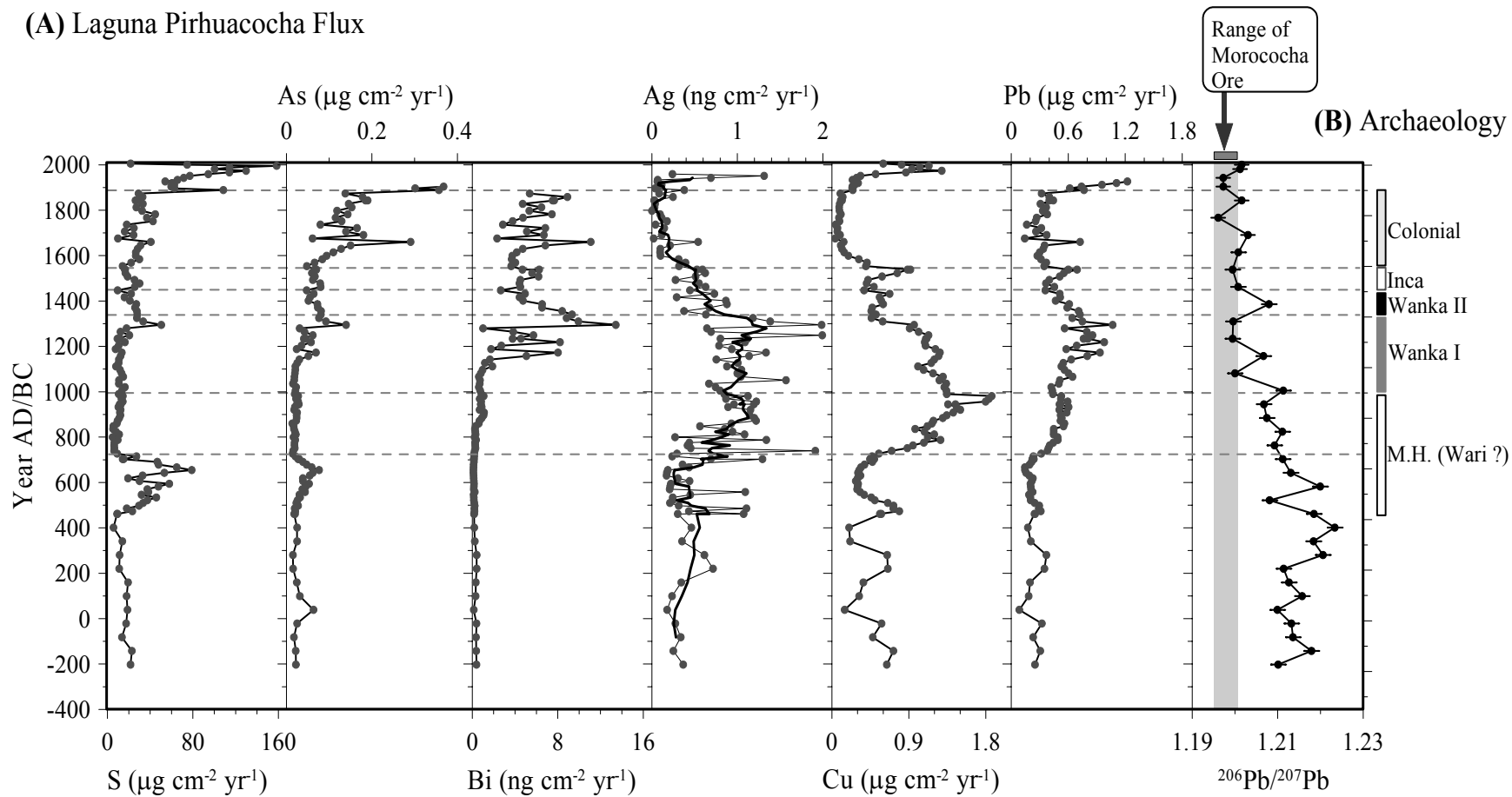


Figure 2.9 (a) Laguna Pirhuacocha elemental flux and $^{206}\text{Pb}/^{207}\text{Pb}$ ratios versus (b) archaeological reconstruction of regional cultural chronology. Periods of metal enrichment are synchronous with social stability in the region as indicated by the archaeological record, suggesting local or regional control of resources. The heavy black line in the Ag profile represents a five-point running average.

This first appearance of metal pollution at Laguna Pirhuacocha coincides with the onset of the Andean Middle Horizon (500 to 1000 AD). The Andean Middle Horizon witnessed the growth and expansion of the largest pre-Incan Peruvian culture, the Wari. Though controversial, there is agreement that Wari was an expansionist state encompassing nearly all of highland Peru (Schreiber, 1992). Since the 1940's a large amount of archaeological research has been carried out in the nearby Mantaro River valley, near the modern day town of Jauja (Figure 2.1). This archaeological research is the closest geographically to the study sites and provides the most applicable record for comparison. However, an almost complete lack of Wari artifacts (let alone Wari metal artifacts) recovered from the study region suggests that the Wari Empire exerted limited influence over local culture history (Earle *et al.*, 1980). Indeed, very few metal artifacts from the Andean Middle Horizon in general have been found (King, 2000). Those that have are predominantly copper or copper alloy and are limited to a relatively few, large archaeological sites (Lechtman, 2002, 2005). For these reasons it remains difficult to ascertain which culture group was smelting at Morococha during the Middle Horizon. However, the close correlation with the emergence of the Wari suggests that even if not directly involved, the Wari may have served as the diffusive mechanism that brought the technology or knowledge necessary to conduct copper metallurgy to the central Andes. The collapse of the Wari polity ca. 1000 AD is correlated with a synchronous reduction in copper (though Cu remains well above background) and a rise in $^{206}\text{Pb}/^{207}\text{Pb}$, suggesting some level of either direct (e.g. state controlled) or indirect (e.g. decreased trade) economic influence over metal extraction from Morococha.

With the collapse of the Wari Empire, regional pre-history can be divided into a series of culturally continuous phases termed "Wanka" (named for the local population who were called Wanka by both the Inca and subsequently the Spanish). During Wanka I (ca. 1000 to 1350 AD),

which was socially stable (Hastorf *et al.*, 1989), populations were egalitarian in nature and were organized into small towns and villages located on valley bottoms (Earle *et al.*, 1980). Wanka I also contains the earliest archaeological evidence for local metallurgy and the earliest metal artifacts found during archaeological excavations date to this period (Howe and Petersen, 1992). Based on the Laguna Pirhuacocha record, metallurgy at this time was increasingly directed towards silver and less so towards copper, as copper steadily declines towards background levels except for a brief increase ~1200 AD. At the same time Ag, Pb, and Bi all increase above previous levels; Ag and Bi reached levels not seen again until the modern era. Many of the silver bearing ores in the area are Bi-rich (Peterson, 1965b) and together with the increase in Ag and Pb, suggest that at the end of the Middle Horizon, the emphasis shifted away from copper and towards silver metallurgy.

A new emphasis on silver metallurgy is also supported by the first appearance of trace metal pollution within Laguna Chipian sediments (Figures 2.6 and 2.10). Sometime between 1000 and 1200 AD, Pb flux increased above a previously stable background. Though Cu also increased at this time, it rapidly leveled off, suggesting an unchanging amount of Cu was volatilized during smelting. Unexpectedly the Ag flux decreases during this period. This may be because by the time metallurgy reached Cerro de Pasco, smelting technologies had advanced enough to limit volatile losses of silver. This intensification (or emergence) of silver smelting occurred about the same time as silver metallurgy began at Cerro Rico de Potosí in Bolivia. Previously, Abbott and Wolfe (2003) concluded that silver metallurgy at Potosí, the largest silver mine in the Americas, began at 1000 AD.

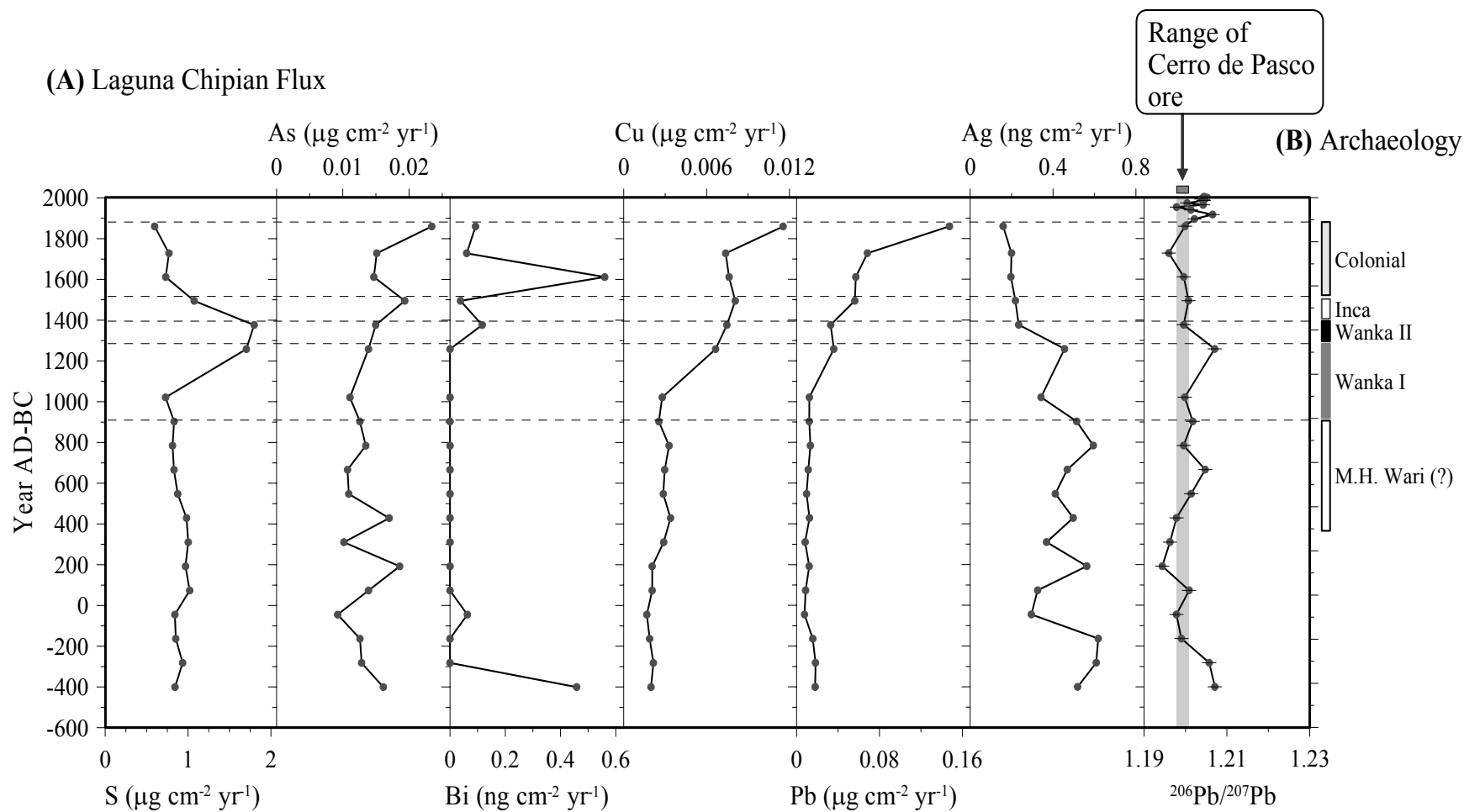


Figure 2.10 (a) Laguna Chipian elemental flux and $^{206}\text{Pb}/^{207}\text{Pb}$ ratios versus (b) regional cultural chronology. After 1000 AD, qualitative trends in metal enrichment at Laguna Chipian correlate to those observed at Laguna Pirhuacocha, suggesting both locations are locally administered.

During the Wanka II phase (1350 to 1460 AD), a dramatic shift in population occurred, with the population aggregated into a few large, dense settlements located on high knolls outside of the valley (Earle *et al.*, 1980). Both the Laguna Chipian and Laguna Pirhuacocha sediment records indicate metallurgy continued during this period, though at reduced levels (Figures 2.9 and 2.10). What might have caused this simultaneous decline in metallurgy at both study sites? One possibility may be the exploitation of alternate ore resources during this period. Alternatively, the archaeological record indicates that during Wanka II strong wealth gradients between elite and commoners developed and warfare erupted (Hastorf, 1990). Seltzer and Hastorf (1990) have previously argued, based on glacial geomorphological evidence, that cooler climatic conditions reduced the land area available for maize cultivation. This in turn may have exacerbated existing social tensions, leading to the establishment of defensive settlements and warfare (Seltzer and Hastorf, 1990). The warfare may have led to competition for ore resources, as well as decreased access to the mines themselves, though this remains speculative. Whatever the cause, the sediment record presented here records a decline in metallurgy during this time period.

The Andean Late Horizon (1460 to 1533 AD) begins with the Inca hegemony and ends with the establishment of Jauja (Figure 2.1) as the capital of Colonial Peru. After Inca conquest, the population was relocated to the valley bottoms and a major Inca administrative site, Huatun Xauxa, was constructed. This site was built in part to serve as a storage facility for food and tribute items including precious metals extracted from the local population as tax (D'Altroy and Hastorf, 1984). Metallurgy at Cerro de Pasco continued under the Inca, though surprisingly not at levels significantly above previous smelting regimens (Figures 2.9 and 2.10). At Laguna Pirhuacocha, Cu and Pb increase while Ag does not, suggesting either technological advances by

Incan metallurgists aimed at minimizing volatile losses of silver, or a resurgence of copper metallurgy. The Inca also initiated the widespread use of tin bronze in the Andes (Lechtman, 1976, 1979, 1980; Owen, 1986). In the central Andes, small amounts of tin were incorporated into all copper and copper-arsenic alloys (Owen, 1986). The tin records from both study sites show no change during the Late Horizon. Therefore, the addition of tin to all copper alloys was likely limited to the late stages of production and was carried out at the local population centers, rather than at the mines themselves, which agrees with the archaeological findings of Howe and Petersen (1992).

Jauja was established as the first capital of Peru after the conquest of the Inca in 1532 AD. Purser (1971) reports that mining at Morococha began shortly after 1600 AD but that Colonial operations ended within a decade or two. The geochemical record appears to faithfully record this brief attempt at metallurgy at Morococha, as a single datum ca. 1650 (representing ~15 years) rises above an otherwise static colonial period (Figure 2.9). However, during colonial times, $^{206}\text{Pb}/^{207}\text{Pb}$ remains low and even decreases coming into equilibrium with published $^{206}\text{Pb}/^{207}\text{Pb}$ ratios for Morococha ore (Gunnesch *et al.*, 1990; Macfarlane *et al.*, 1990). This suggests some anthropogenic Pb pollution continued. Purser (1971) reports that during the early 1800's indigenous smelting of argentiferous galena was carried out on the hilltops using traditional *huyaras*. This metallurgical activity maintained a low $^{206}\text{Pb}/^{207}\text{Pb}$ until the onset of the 20th century.

Cerro de Pasco was “discovered” by Colonial metallurgists in 1630 and was rapidly developed (Fisher, 1977). It was the second most important silver mine in Colonial Peru and after Cerro Rico de Potosí was the largest producer of silver in the New World (Purser, 1971; Fisher, 1977). As surface ores were quickly depleted, the ground beneath the mine became

honeycombed with underground workings, and mercury amalgamation took over as the predominant silver extractive process (Fisher, 1977). Mercury amalgamation was brought to Peru from Mexico and facilitated the extraction of silver from lower grade audits (Craig, 1989). The sediment record suggests some smelting at Cerro de Pasco continued during this period, as Pb steadily increases.

2.5.2 The modern era

With the building of the central Peruvian railway in early 20th century, the central Andean mining districts developed rapidly. Metal emissions from operations at Morococha, and presumably the large-scale smelter at nearby La Oroya (Figure 2.1) elevated the Pb in the sediments of Laguna Pirhuacocha to $>2,500 \mu\text{g g}^{-1}$ (Figure 2.6). Concentrations of Pb, Cu and Bi peak ca. 1980 AD before subsequently declining, while Ag and As reach a maxima in the uppermost samples, concurrent with a decline in sediment S. The level of contamination at Laguna Chipian is lower and Pb, Cu, Bi and As have declined in recent decades (Figure 2.8).

2.6 CONCLUSION

The sediment records presented here yield two distinct regional histories of environmental pollution caused by smelting. Though the silver deposits at Morococha were reportedly first worked by colonial metallurgists in the 17th century, the Laguna Pirhuacocha sediment record suggests that metallurgy at Morococha began at least a millennium prior, ca. 500 AD. Early metallurgy at Morococha appears to have been aimed at copper and copper alloys. A possible link to the Wari state is suggested as the onset of metallurgy is temporally synchronous

with the emergence of the Wari Empire. The expansion of Wari outside of its imperial core may have been driven, in part, by a desire to extract prestige goods such as metals from local populations (Jennings and Craig, 2001). Implicit to this hypothesis is the suggestion that the manufacture of prestige goods was largely independent of state oversight. The increase in post-Wari metallurgical activity supports this conclusion, as the intensity of metallurgical activity was controlled at the local or regional level. This suggests that different metallurgical centers had unique trajectories for development.

3.0 LATE HOLOCENE HISTORIES OF ATMOSPHERIC LEAD DEPOSITION FROM THE CENTRAL ANDES: INSIGHT INTO PRE-HISPANIC METALLURGY

3.1 INTRODUCTION

Natural archives can be used to document the timing and relative magnitude of atmospheric lead (Pb) deposition. Such archives include: ice cores (Rosman *et al.*, 1994; Hong *et al.*, 1996), peatlands (Shotyk *et al.*, 1996; Martinez Cortizas *et al.*, 2002), marine sediments (Véron *et al.*, 1987), lichens (Doucet and Carignan, 2001; Carignan *et al.*, 2002) and lake sediments (Bindler *et al.*, 2001; Renberg *et al.*, 2002). These archives chronicle pre-historic Pb pollution histories associated with metallurgical activity at regional to hemispheric scales, depending on the sensitivity of the medium. However, few studies have quantified Pb pollution at local to regional scale (e.g. Monna *et al.*, 2004; Baron *et al.*, 2005), while only two other studies have examined local scale Pb pollution associated with pre-Hispanic metallurgical activity in the Andes (Abbott and Wolfe, 2003), despite a rich history of metallurgical development prior to Hispanic conquest (Lechtman, 1980).

We measured weakly-bound Pb in four lake cores spanning the middle to late-Holocene to reconstruct local to regional histories of anthropogenic Pb pollution due to smelting. Lead input to lake sediment can be used as a proxy for smelting intensity because there is both historical and archeological evidence for the use of argentiferous galena [(Pb, Ag)S; locally known as *soroche*] during the smelting process of silver-rich ores, which was conducted in clay-

lined, wind-drafted furnaces called *huayaras* (Bakewell, 1984). In addition, Pb has the advantage of not suffering from diagenetic overprinting in lake sediments (Brännvall *et al.*, 2001; Gallon *et al.*, 2004). Here, we present four late Holocene histories of Pb pollution due to smelting from the Peruvian and Bolivian Andes. We combine the previously published Laguna (L.) Lobato Pb record from Cerro Rico de Potosí, Bolivia (Abbott and Wolfe, 2003) with a new geochemical record from L. Taypi Chaka Kkota, Bolivia (Abbott *et al.*, 1997b) and two new geochemical records from L. Chipian and L. Pirhuacocha, Peru.

3.2 STUDY SITES

Lake characteristics and limnological measurements are summarized in Table 1, while the location of the study sites is shown in Figure 1.

Table 3.1 Location of study sites and lake characteristics.

Lake	Latitude	Longitude	Lake area (m ²)	Catchment area (m ²)	Elevation (m)	Depth (m)	pH
L. Chipian	10° 43' 08" S	76° 10' 12" W	0.1	2.8	4324	3	11
L. Pirhuacocha	11° 31' 24" S	76° 04' 50" W	0.1	3.1	4520	19	7.8
L. Taypi Chaka Kkota	16° 10' 30" S	68° 19' 15" W	0.3	7.4	4550	11	7.5
L. Lobato	19° 38' 20" S	65° 41' 50" W	0.2	3.9	4640	11	7.5

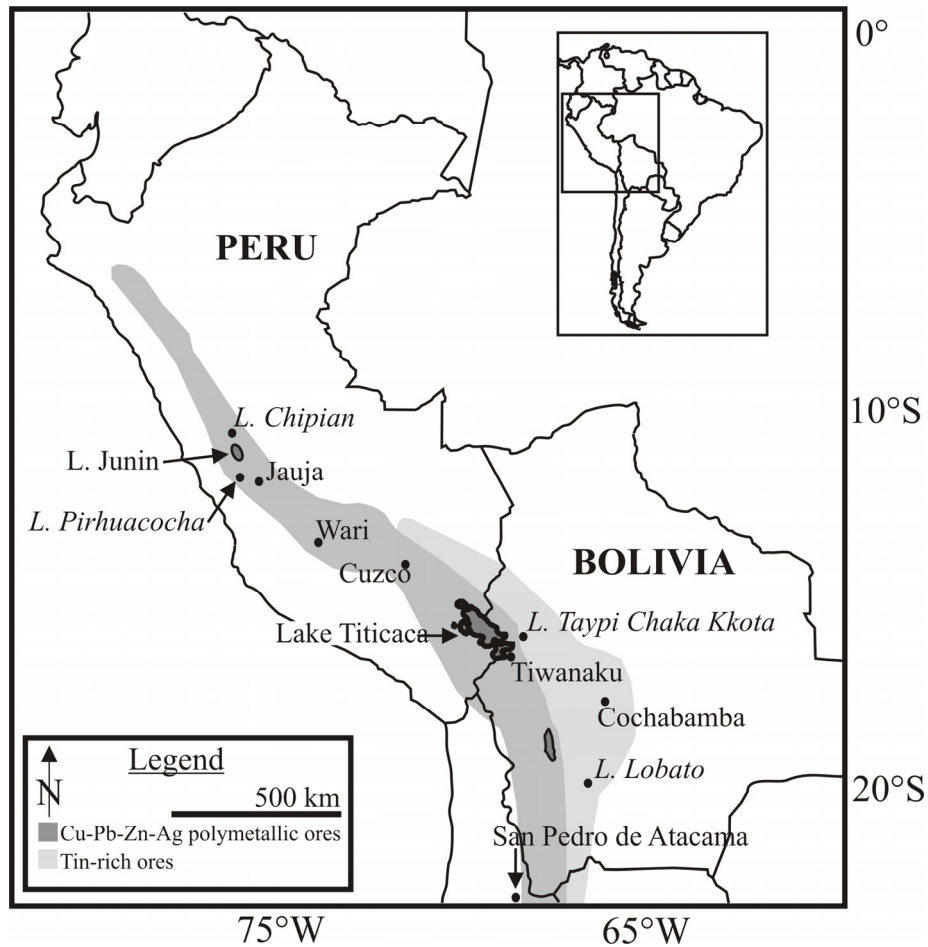


Figure 3.1 Map of study lakes (*italics*) as well as archaeological sites and towns discussed in text. Arsenic-rich polymetallic orebodies as well as tin-rich ore deposits are noted on the map.

Cerro de Pasco is located in the Junin district on the Peruvian *altiplano* east of the continental divide and west of the Cordillera Oriental. The ore bodies at Cerro de Pasco are associated with Tertiary volcanic vents located in the core of a non-plunging anticline of Devonian age (Ward, 1961). In addition to native silver, the principle ores contain combinations of arsenopyrite (FeAsS), aramayoite [Ag(Sb, Bi)S₂], chalcopyrite (CuFeS₂), enargite (Cu₃AsS₄), argentiferous galena [(Ag, Pb)S], tennantite (Cu₁₂As₄S₁₃), grantonite (Pb₉As₄S₁₅), and sphalerite [(Zn, Fe)S] (Ward, 1961; Einaudi, 1977). Cerro de Pasco was the second largest producer of

silver in Colonial Peru (Purser, 1971; Fisher, 1977), and is estimated to have contained one-thousand tons of silver, four million tons of zinc, two million tons of lead and lesser amounts of gold and bismuth prior to Colonial exploitation (Peterson, 1965a; Einaudi, 1977).

L. Chipian ($10^{\circ} 43' S$, $76^{\circ} 10' W$) rests on carbonate terrain of Jurassic age ~9 km southeast of Cerro de Pasco. L. Chipian is a small (0.12 km^2), shallow (3 m), alkaline (pH=10) lake occupying a catchment of 2.81 km^2 . The lake sits at the apex of a small valley, which funnels surface winds blowing off the *altiplano* from the west. A large collection of Colonial smelters and grinding wheels (locally called *batans*) are located in the valley bottom below L. Chipian. Also located very near to the smelters are a number of small excavations believed to be Colonial pit mines.

The Morococha mining region is located in the Junin district of the western Cordillera. The mining area sits in the Río Puará river valley and is situated over replacement bodies, such as mantos, chimneys and skarns (Gunnesch *et al.*, 1990). In addition to native silver, the richest ores at Morococha contain combinations of anhydrite (CaSO_4), barite (BaSO_4), bourmonite (CuPbSbS_3), arsenopyrite, chalcopyrite, emplectite (CuBiS_2), enargite, galena, matildite (AgBiS_2), proustite ($\text{Ag}_3\text{As}_3\text{S}_3$), sphalerite, stromeyerite (AgCuS), and tennantite (Ward, 1961; Einaudi, 1977). Morococha was reportedly discovered during the 17th century by Colonial metallurgists (Purser, 1971).

Located 11 km northeast of modern silver mining operations at Morococha (Figure 1b), L. Pirhuacocha ($11^{\circ} 31' S$, $76^{\circ} 04' W$) occupies Cretaceous carbonate terrain. The lake lies within a cirque depression in a small valley located perpendicular to the Río Puará river valley. The lake is circumneutral and is 18 m deep. The lake is small (0.05 km^2) and occupies a non-glacial catchment of 3.14 km^2 . L. Pirhuacocha drains to the east during the wet season

(December to March) through a small creek, and a small littoral bench sits at the mouth of this creek. Surface winds driven by daytime heating blow predominantly from the west rising up the valley during the day and sink back down the valley at night.

In Bolivia, L. Taypi Chaka Kkota is a glacially-fed lake situated in the Río Palcoco valley on the western side of the Cordillera Real (Abbott *et al.*, 1997b). Though L. Taypi Chaka Kkota is not located near any modern mining activities, it was included in this study because it lies ~40 km northeast of the Tiwanaku archaeological zone. Metal artifacts have been recovered during archaeological excavation at Tiwanaku and it was an important area for cultural development in Andean pre-history (Lechtman, 2002). Finally, L. Lobato sits 6 km east of Cerro Rico de Potosí, the largest silver deposit of the Bolivian tin belt (Abbott and Wolfe, 2003). Cerro Rico lies within a zone of xenothermal mineralization related to mid-Tertiary intrusions. In addition to native silver, the richest ores contain combinations of acanthite (Ag_2S), andorite ($\text{PbAgSb}_3\text{S}_6$), chlorargyrite (AgCl), matildite (AgBiS_2), miargyrite (AgSbS_2), pyrargyrite (Ag_3SbS_3), and tetrahedrite [$(\text{Ag, Cu, Fe, Zn})_{12}\text{Sb}_4\text{S}_{13}$] (Abbott and Wolfe, 2003).

None of the study lakes have any hydrological connection with mining activities, and are propitiously suited to record atmospheric fallout of Pb volatilized during smelting.

3.3 METHODS

3.3.1 Core collection and chronology

The sediment cores were recovered from the deepest points of the lakes using coring devices which preserve an intact sediment-water interface. A minimum of 15-cm of the uppermost sediment from each core was extruded in the field at 0.5 cm resolution to eliminate

disturbance in the uppermost sediments. The sediment cores and chronological methods used to reconstruct age-depth relationships have been described in detail elsewhere but are summarized here as well (Abbott *et al.*, 1997b; Abbott and Wolfe, 2003; Chapter 2). The upper sections of every core, except for L. Taypi Chaka Kkota, were dated using excess ^{210}Pb activities ($t_{1/2}=22.3$ years) measured by α -spectroscopy. A constant rate of supply (CRS) age model was applied to the ^{210}Pb activities at L. Chipian and L. Lobato and a constant initial concentration (CIC) age model was applied at L. Pirhuacocha (Appleby, 2001). To temporally constrain changes beyond the limit of ^{210}Pb dating, Accelerator Mass Spectrometry (AMS) ^{14}C dates were obtained on terrestrial and aquatic macrofossils and charcoal, all of which are reported in Table 3.2. Radiocarbon dates were converted to calendar years AD using the program Calib 5.0 (Reimer *et al.*, 2004). The dates obtained on aquatic macrophytes at L. Pirhuacocha are reported but were not included in the construction of the age model due to a fluctuating hard-water reservoir effect. At all of the study sites, linear regression between individual ^{14}C dates and the base of ^{210}Pb chronologies allows for the development of composite chronological models.

Table 3.2 Table of ^{14}C dates used in this study.

Lake	Lab ID	Depth (cm)	^{14}C age (BP)	Year AD Range (2 σ)	$\delta^{13}\text{C}$ (‰)	Median Date AD/BC	Material
L. Chipian	UCI-9339	26-28	400 \pm 30	1437-1522	-12.4	1480	Charcoal
	UCI-9340	35-37	1055 \pm 45	886-1042	-11.6	980	Charcoal
L. Pirhuacocha	UCI-9333	8-9	615 \pm 30	1294-1401	-31.5	1348	Aquatic macro
	UCI-19865	30.5-31	840 \pm 30	1155-1265	-24.2	1203	Aquatic macro
	UCI-9334	36.5-38	1030 \pm 20	983-1026	-24.8	1005	Charcoal
	UCI-18664	48-48.5	1245 \pm 20	685-784	-31.8	739	Aquatic macro
	UCI-9335	50-51	1285 \pm 20	671-730	-18.3	715	Charcoal
	UCI-19866	58-59	1000 \pm 30	983-1052	-21.6	1025	Aquatic macro
	UCI-19867	77-77.5	1615 \pm 25	397-534	-35.6	456	Aquatic macro
	UCI-19868	84-84.5	1615 \pm 25	397-534	-33.7	456	Aquatic macro
UCI-18663	90	940 \pm 20	1031-1155	-31.9	1098	Aquatic macro	
L. Taypi Chaka Kkota	CAMS-4980	30.5	1470 \pm 80	412-684	NM	574	<i>Isoetes</i> macrofossil
	CAMS-11067	49.5	2290 \pm 60	511-191 BC	NM	328 BC	<i>Isoetes</i> macrofossil
	CAMS-11068	52.5	2880 \pm 60	1223-909 BC	NM	1069 BC	<i>Isoetes</i> macrofossil
	CAMS-5749	63.5	3690 \pm 70	2235-1894 BC	NM	2082 BC	<i>Isoetes</i> macrofossil
	CAMS-5748	89.5	5110 \pm 60	4004-3766 BC	NM	3884 BC	<i>Isoetes</i> macrofossil
L. Lobato	OS-18622	60	1060 \pm 40	893-1026	-17.6	979	Macrofossil
	OS-18623	72.5	1270 \pm 50	661-872	-17.5	743	Macrofossil

NM = not measured

3.3.2 Lead geochemistry

Cores were subsampled at 0.5-cm, 1-cm, and 2-cm intervals for L. Pirhuacocha, L. Lobato, L. Taypi Chaka Kkota and L. Chipian respectively. Sediment Pb was extracted from 0.1 to 1.0 g of homogenized, freeze-dried sediment using 10 ml of 1.6 M Optima grade HNO₃ at room temperature for 24 hours. This weak extraction procedure deliberately targets weakly-bound Pb adsorbed to organic and inorganic surfaces, and not those associated with the mineralogy of sediment inorganic constituents (Shirahata *et al.*, 1980; Ng and Patterson, 1982; Hamelin *et al.*, 1990; Kober *et al.*, 1999). Graney *et al.* (1995) reported that the strength and acid used for the extraction has limited impact on the amount of Pb leached. Therefore, this extraction obtains most, if not all, of the anthropogenic Pb added to the sediment. An inductively coupled plasma-atomic emission spectroscopy (ICP-AES Spectroflame-EOS) was used to measure Pb concentration for samples from Lagunas Chipian, L. Taypi Chaka Kkota and Pirhuacocha. A Perkin-Elmer Sciex Elan 6000 inductively coupled plasma-mass spectrometer (ICP-MS) was used for Laguna Lobato. Lead concentrations are reported as $\mu\text{g Pb g}^{-1}$ dry sediment mass. Instrument detection limits (IDL) were $5 \mu\text{g g}^{-1}$ for L. Chipian and L. Pirhuacocha, $2 \mu\text{g g}^{-1}$ for L. Taypi Chaka Kkota and $0.0005 \mu\text{g g}^{-1}$ for L. Lobato.

Though concentration data are commonly used to interpret sediment geochemical records, such an operation must be undertaken with care as concentrations may be enhanced or diluted by variations in mineral matter or major elemental fluxes as well as changes in sediment compaction (Norton and Kahl, 1991). Flux was calculated for each record as the products of Pb concentration ($\mu\text{g g}^{-1}$), sediment accumulation rate (cm year^{-1}) and core dry bulk density (g cm^{-3}) to correct for such biases.

3.4 RESULTS

Lead input, calculated as concentration (Figure 3.2) or flux (Figure 3.3), is low and invariable at all of the study sites prior to 500 AD. These represent background levels of Pb accumulation for each watershed. In addition, 26 samples from L. Taypi Chaka Kkota and 15 samples from L. Lobato, spanning the middle to late-Holocene, were measured for Pb concentration in order to determine if regional changes in climate or hydrology impacted the natural flux of Pb to these study sites. The results from these analyses, shown in Figure 3.4, indicate that, despite evidence for severe periods of aridity and pronounced hydrologic change (Thompson *et al.*, 1985; Abbott *et al.*, 1997a; Abbott *et al.*, 2000), there was no significant change in the flux of nonpollution Pb to the study sites.

The first evidence for Pb enrichment at any of our study sites occurs ca. 500 AD at L. Taypi Chaka Kkota rising to $\sim 25 \mu\text{g g}^{-1}$. Though this elevated Pb concentration is within the range of background variability at L. Lobato and L. Pirhuacocha, the stable flux of nonpollution Pb to the lake demonstrates that this Pb is anthropogenic in origin. The next increase in Pb flux occurs at L. Pirhuacocha, as Pb increases two-fold over background levels ca. 700 AD (Figure 3.3; Chapter 2). After 1000 AD, Pb at L. Lobato increases followed by an increase at L. Chipian after ~ 1200 AD. These Pb enrichment events cannot be due to a hemispheric or occur at different times, and at different core depths.

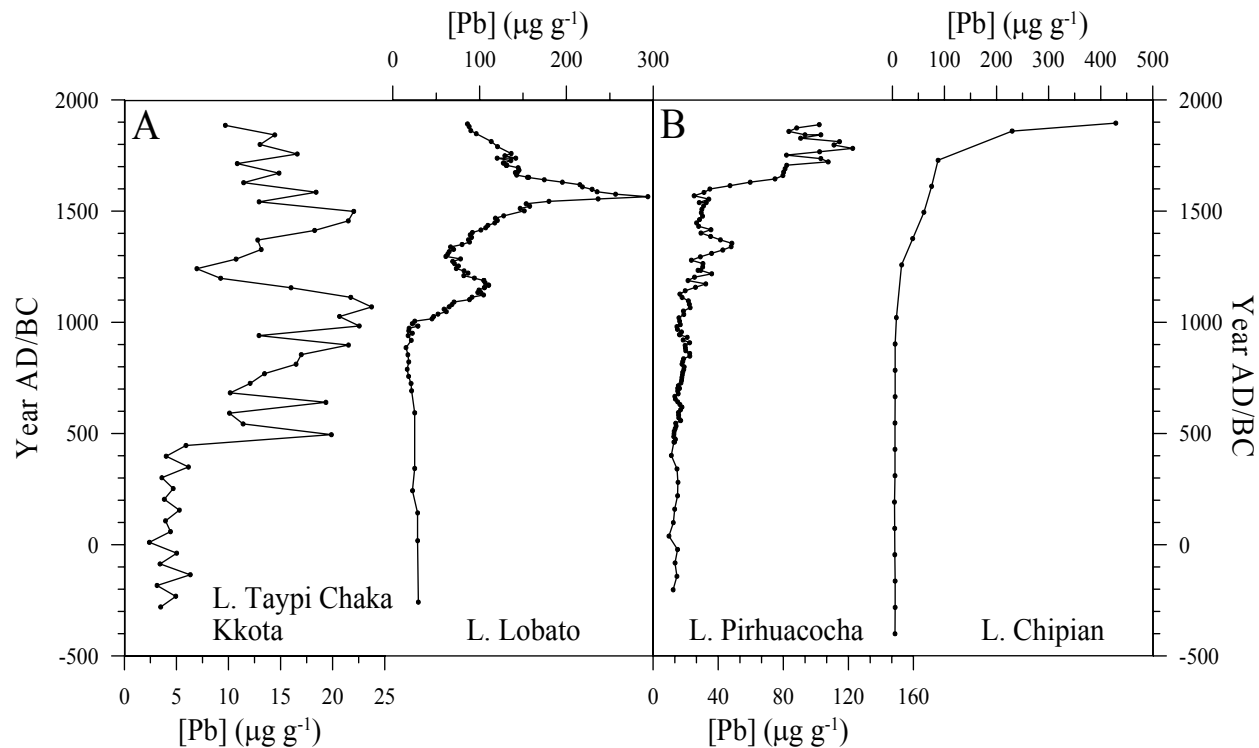


Figure 3.2 Stratigraphic profiles of Pb concentration from (a) Bolivian and (b) Peruvian study sites. The uppermost samples dating to the 20th century have been removed to highlight pre-industrial changes down-core.

Pb flux Andes

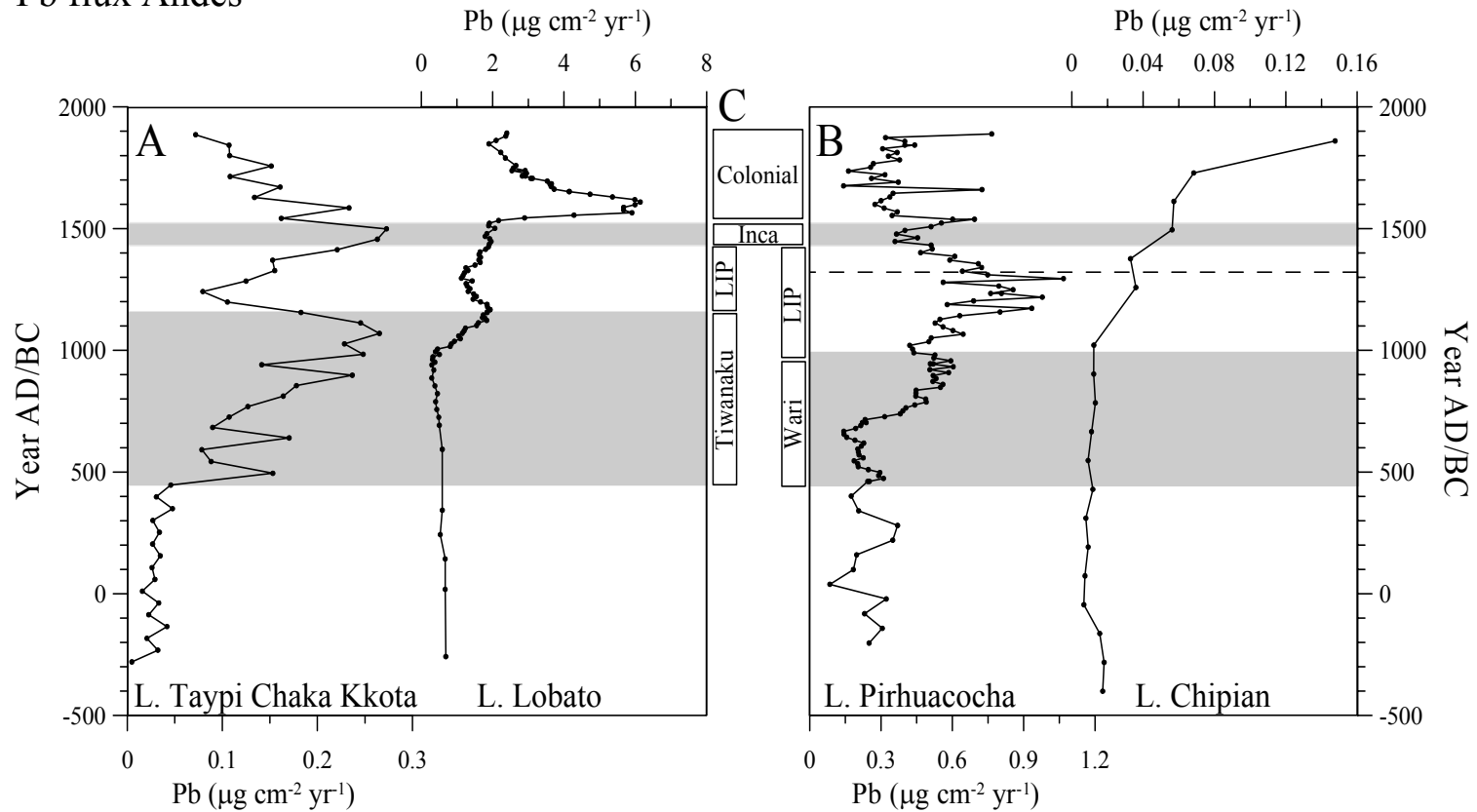


Figure 3.3 Stratigraphic profiles of Pb flux from (a) Bolivian and (b) Peruvian study sites shown alongside (c) regional cultural chronology. The dashed line in (b) represents the division of the Late Intermediate Period (LIP) into the Wanka I and Wanka II cultural phases (see text). As in Figure 3.2, the uppermost samples dating to the 20th century have been removed to highlight pre-industrial changes down-core.

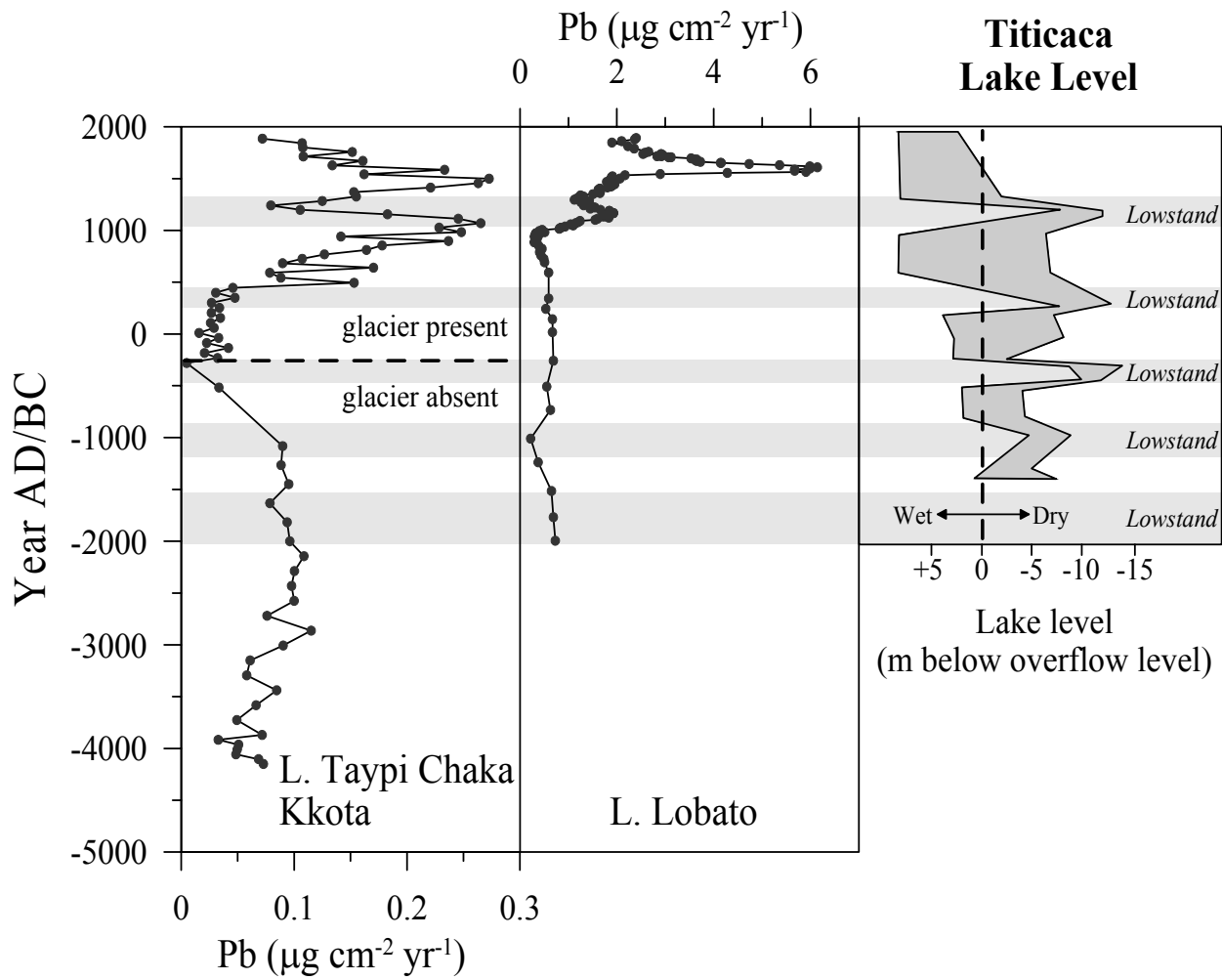


Figure 3.4 Prior to 500 AD at L. Taypi Chaka Kkota and 1000 AD at Lobato, the natural flux of Pb to each lake was stable and low representing pristine Pb accumulation levels. In addition, both Pb records are stable during pronounced periods of aridity as demonstrated by the lake level reconstruction for Lake Titicaca from Abbott et al. (1997a).

3.5 DISCUSSION

3.5.1 The Middle Horizon (~500 to 1000 AD)

The onset of Pb pollution ca. 500 AD at L. Taypi Chaka Kkota coincides with the rise of the Tiwanaku culture. The Tiwanaku were based on the southern shores of Lake Titicaca but also expanded to include colonies along the southwest coast of Peru, enclaves near Cochabamba in the Bolivian Andes, and they engaged in trade as far south as San Pedro de Atacama, Chile (Figure 3.1) (Rodman, 1992; Kolata, 1993; Moseley, 2001; Stanish, 2002). An array of bronze artifacts has been recovered during archaeological excavations within the Titicaca basin, suggesting a bronze-based metal industry of considerable scope (Lechtman, 2002). The L. Taypi Chaka Kkota sediment record faithfully records this metallurgical industry. After 700 AD, smelting within the Titicaca basin increases through time, before precipitously dropping to background between 1100 and 1200 AD. This rapid decrease to background levels would suggest metallurgy within the Tiwanaku basin came to an abrupt halt following the collapse of the Tiwanaku culture on the *altiplano*. Though controversial, the collapse of the Tiwanaku has been linked to a pervasive drought ca. 1040 to 1400 AD which forced the abandonment of raised field agriculture (Kolata, 1993; Binford *et al.*, 1997). The lake level of Titicaca dropped by as much as 6 m between 1100 and 1250 AD (Abbott *et al.*, 1997a), when precipitation declined as recorded by the Quelccaya ice core (Thompson *et al.*, 1985). However, this view has been challenged as the abandonment of the Tiwanaku center, the loss of raised field agriculture, and the increase in climatic aridity are independent events; causation, rather than correlation, has yet to be convincingly demonstrated (Williams, 2002; Isbell, 2004; Callaway, 2005; Owen, 2005). Moreover, Owen (2005) has recently proposed that collapse of the Tiwanaku colonies in

southwest Peru may have occurred as early as the late 10th century AD, preceding the collapse of the Tiwanaku heartland by as much as 200 years. Curiously, the L. Taypi Chaka Kkota sediment record records a decline in Pb pollution during the late 10th century AD, though this is a single datum (Figure 3.3). Alternatively, Kolata (2003:194) has proposed a dramatic reorientation of the Tiwanaku state during the 10th century by “warrior elites” with a collapse occurring somewhat later (ca. 1100 to 1200 AD). Whichever the case, dramatic changes to the Tiwanaku state occurred ca. 1000 AD. The L. Taypi Chaka Kkota record would appear to support a later date for abandonment of the *altiplano*, as the proposed full collapse of the Tiwanaku polity during the 12th century is matched by a corresponding decline to background of Pb pollution.

Lead pollution at Potosí began after 1000 AD, post-dating metallurgy in the Lake Titicaca basin by ~500 years. Smelting activity at Potosí increases until ~1180 AD, and declines thereafter. We propose two possible explanations to explain this later onset of metallurgy at Cerro Rico de Potosí. The first possibility is that metallurgical activity at Potosí was under the direct control of the Tiwanaku culture. This was the conclusion reached previously by Abbott and Wolfe (2003) and would support the notion of a large expansion of the Tiwanaku Empire ca. 1000 AD. Alternatively, Owen (2005) has proposed that the collapse of the Tiwanaku colonies generated a “victim/refugee” diaspora. This diaspora would have spread Tiwanaku peoples, culture, and presumably knowledge of smelting over a wide geographical area and may have brought smelting to Potosí (Owen, personal communication). Discerning which of these two possibilities occurred is difficult using our sediment records; however, from 1100 to 1200 AD, Pb at L. Taypi Chaka Kkota decreases while Pb at L. Lobato increases. This in combination with a complete lack of smelting at Potosí during the height of Tiwanaku culture (i.e. 500 to 1000

AD), would seem to support the idea that smelting at Potosí is related to the collapse of the Tiwanaku state, rather than its expansion.

The first indication of Pb pollution in Peru is found within Pirhuacocha sediment ca. 700 AD (Figure 3.3). This increase coincides temporally with the expansion of the Wari Empire, who expanded out of the Ayacucho valley, Peru (Schreiber, 1992). However, archaeological excavations conducted near the modern city of Jauja (Figure 3.1) have yielded almost no Wari artifacts, suggesting little Wari influence over local resource exploitation (Earle *et al.*, 1980). However, the synchrony between the decline in Pb pollution at Morococha and the collapse of the Wari state ca. 1000 AD suggests that metallurgy at Morococha was either indirectly (i.e. through trade) or directly linked to the larger Wari polity.

3.5.2 The Late Intermediate Period (~1000 to 1450 AD)

During the subsequent Late Intermediate Period, which separated Tiwanaku and Inca imperial regimes, decentralized polities arose within the Lake Titicaca basin (Bauer and Stanish, 2001). At L. Taypi Chaka Kkota, Pb flux decreases to background ($\sim 0.7 \mu\text{g cm}^2 \text{ yr}$) by 1250 AD. At L. Lobato, Pb flux begins to decrease ~ 1200 AD, though remains well above background levels. At both study sites Pb flux begins to increase between 1200 and 1300 AD, suggesting increases in metallurgical activity during the Late Intermediate Period in Bolivia. These increases occurred in the absence of any large scale state, suggesting metallurgical production was conducted at the household level and was locally administered.

The Late Intermediate Period in Peru reveals a somewhat different pattern than that observed in Bolivia. After a very brief decline in Pb ~ 1000 AD, Pb flux at Pirhuacocha begins to increase, and by the late 13th century reaches the highest pre-industrial level recorded. The late

13th century also contains the earliest evidence for Pb enrichment within L. Chipian sediment (Figures 3.2 and 3.3). From ~1300 to 1450 AD, Pb flux subsequently decreases at L. Pirhuacocha while remaining stable at L. Chipian.

The Late Intermediate Period of central Peru can be subdivided into two culturally continuous phases termed Wanka I and Wanka II (named for the local population who were called Wanka by both the Inca and the subsequent Spanish). During Wanka I (ca. 1000 to 1350 AD), which was climatically warm (Seltzer and Hastorf, 1990) and socially stable (Hastorf *et al.*, 1989), populations were egalitarian in nature and were organized into small towns and villages located on valley bottoms (Earle *et al.*, 1980). During the subsequent Wanka II phase (ca. 1350 to 1460), a dramatic shift in population occurred, with the population aggregated into a few, large, dense settlements located on high knolls outside of the valley (Earle *et al.*, 1980). The L. Pirhuacocha and L. Chipian Pb pollution histories suggest that smelting increased during the early part of the Late Intermediate Period (Wanka I) and decreased or remained static during the latter part (Wanka II).

As observed in Bolivia, the increase in metallurgy during the Late Intermediate Period occurs in the absence of any large state or polity. However, Pb pollution at L. Pirhuacocha and L. Chipian declines during the latter half of the Late Intermediate Period, just as it is increasing at both L. Taypi Chaka Kkota and L. Lobato. This difference emphasizes the importance of local rather than regional or state-level control of resources in both central Peru and within Bolivia.

3.5.3 The Late Horizon (~1450 to 1530 AD)

The onset of the Late Horizon ca. 1450 AD is defined by the onset expansion of the Inca hegemony across the Peruvian and Bolivian Andes and all four of the study sites examined here

were eventually incorporated into the Inca Empire. In Bolivia, metallurgy on the *altiplano* peaks during the Inca hegemony, surpassing previous levels of Pb pollution at L. Taypi Chaka Kkota (Figures 3.2 and 3.3). Metallurgy at Potosí also continues during this period, though not surpassing levels attained during the Middle Horizon and Late Intermediate Period.

3.5.4 The Colonial era (1532 to 1900 AD)

The colonial era began with the conquest of the Inca Empire in 1532 AD. The Spanish Conquistadores quickly melted down all precious metals before turning their attention to the mines themselves. Potosí was the first Inca mine to be developed by the Spanish after conquest, and in the 27 years following Spanish rule, thousands of *huyaras* adorned the mountainside. Their collective Pb emissions elevate Pb flux at L. Lobato to over $6 \mu\text{g cm}^{-2} \text{ yr}^{-1}$, sixteen times the natural flux of Pb (Figure 3.3). L. Lobato also faithfully tracks the subsequent adoption of mercury amalgamation as the primary extractive technique (Abbott and Wolfe, 2003), leading to a reduction in Pb emissions. The Pb record tracks this technological shift away from direct smelting of silver ores.

With the exhaustion of silver-rich surface ores, a new search for silver deposits began and new mines were developed. With its opening in 1630 AD, Cerro de Pasco rapidly became the second largest producer of silver in Colonial Peru (after Potosí). Due to the lower grade of surface ores at Cerro de Pasco, mercury amalgamation was the favored technique for silver extraction (Fisher, 1977) and as a result Pb flux largely remains unchanged during this period (Figure 3.3). Although mining at Morococha began shortly after 1600 AD, however, Colonial operations ended within a decade or two (Purser, 1971). The geochemical record faithfully

records this brief attempt at metallurgy, as a single datum ca. 1650 (representing ~15 years) rises above an otherwise flat Colonial period.

3.6 CONCLUSION

These results demonstrate an asynchrony of Colonial and pre-Colonial Pb emissions between metallurgical centers. This would suggest different mining centers in the Andes had unique trajectories for development. In Bolivia, periods of metallurgical activity coincide with the climax of the Tiwanaku and Inca Empires. The L. Taypi Chaka Kkota record would also suggest that the Tiwanaku continued to exist on the *altiplano* and produce metals into the 12th century AD, supporting a later date for the collapse of the Tiwanaku heartland. In the central Peruvian Andes, metallurgy developed somewhat later and independent of state oversight and is instead coupled to local culture history.

The observation that Pb pollution began almost synchronous at both Cerro Rico de Potosí and Cerro de Pasco, historically the two largest silver mines in South America, is unexpected. This may be due to a technological development which occurred ca. 1000 AD, perhaps the development of the *huyara* or the use of *soroche*. Alternatively, the arrival of smelting may be simply due to an Andean diaspora following the collapse of Wari and Tiwanaku (Owen, 2005). Additional cores with higher temporal resolution will be needed to fully constrain when smelting began at Cerro de Pasco and to shed further light on the issue.

The records presented here convincingly demonstrate the contribution that natural archives can make to the archaeological record corroborating earlier research by Abbott and Wolfe (2003). If pre-Inca Andean smelting technologies were anything like the *huyaras*

described by the conquistadors at the time of conquest, they are likely to leave little trace in the archaeological record (Van Buren and Mills, 2005). Lakes are ubiquitous across the Andean landscape and therefore offer an independent method for local-scale reconstructions of ancient metallurgical activity where no other records exist.

4.0 THESIS CONCLUSION

This thesis is the culmination of two years of research aimed at reconstructing pre-Hispanic metallurgy in Peru and Bolivia using natural archives. It was found that geochemical and isotopic data faithfully preserve metallurgical signals at local to regional scales, corroborating earlier findings from Bolivia (Abbott and Wolfe, 2003). This is only the second study aimed at reconstructing pre-Hispanic atmospheric pollution in the Andes, and the first to be conducted in Peru. Lakes are ubiquitous across the Andean chain, and their sediment records offer a unique opportunity to supplement cultural material remains.

4.1 FUTURE RESEARCH

A number of opportunities exist to expand on the sediment records presented in this thesis. The obvious first step is to incorporate additional records from other known mining areas to gain a broader perspective of both natural and anthropogenic metal enrichments through time. This work should incorporate quantitative measurements of as many elements as possible, in combination with measurements of stable Pb isotopes, which are shown here to be sensitive indicators of local-scale pollution in the Andes. With additional precision, isotopic ratios involving ^{204}Pb – the least abundant Pb isotope – may shed light on technological shifts in smelting, or the incorporation of new ore resources through time.

Another avenue for exploration would incorporate sediment biogeochemical and ecological records as indicators of environmental change. Carbon, nitrogen and sulfur isotopic data would shed light on possible biogeochemical impacts, while diatom enumeration offers a powerful approach to reconstructing ecological impacts of early pollution. Diatoms are unicellular algae with siliceous cell walls, which are readily preserved in lake sediments. They are sensitive indicators of environmental change and may be more sensitive to changing metal burdens in lake waters than sediment metal profiles, as some metals are vertically mobilized in the sediment column as a consequence of changing redox conditions (Kauppila, 2006).

Potential also exists to incorporate analyses of sediment mercury (Hg). Huancavelica, in the central Andes of Peru, was the second largest producer of mercury during the Colonial era, supplying Bolivia, Peru and Mexico with the mercury needed for amalgamation. Mercury is of concern because of its long atmospheric residence time (1 to 2 years) and its ability to bioaccumulate in the form of methylmercury. Between 1580 and 1900 AD, annual loss of Hg within Colonial silver mines are estimated at ~612 tons/year, roughly 196,000 tons of Hg over the 320 year period (Nriagu, 1994). Given Hg's long atmospheric residence time, this level of pollution should be observable on a global scale. However, the few studies conducted have not revealed any detectable Colonial Hg pollution. Therefore, either previous estimates of Hg volatilization must be grossly in error, or the Hg associated with Colonial mining was not circulated globally but remained within South America. A set of sediment cores from Huancavelica (the source of the Hg) in combination with lake cores from the largest of the Colonial silver mines, would be the logical first step towards addressing this issue.

APPENDIX A

TABLE OF LAKES STUDIED

Lake	Core	Core Length / Amt Extruded (cm)	Latitude	Longitude	Lake Area (km ²)	Catchment Area (km ²)	Core Dated (²¹⁰ Pb / ¹⁴ C)
Larga	A05 HC	75 / 15	07° 56' S	78° 01' W	NC	NC	¹⁴ C
Hualgayoc 1	A05 HC	90 / 15	06° 47' S	78° 38' W	NC	NC	N/A
Hualgayoc 2	A05 HC	118 / 18	06° 42' S	78° 38' W	0.07	1.21	¹⁴ C & ²¹⁰ Pb
Chipian	A05 HC	62 / 62	10° 43' S	76° 10' W	0.12	2.81	¹⁴ C & ²¹⁰ Pb
Pirhuacocha	A05 HC	92 / 28	11° 31' S	76° 04' W	0.05	3.14	¹⁴ C & ²¹⁰ Pb
Sausacocha	A05 HC	98 / 15	07° 47' S	77° 59' W	NC	NC	N/A
Quiruvilla	A05 HC	105 / 15.5	07° 56' S	78° 15' W	NC	NC	N/A
Lucre	A04 HC	176 / 0	13° 62' S	71° 74' W	NC	NC	N/A
	B04 HC	62 / 62			NC	NC	¹⁴ C
Sojococha	A04 HC	87 / 30	13° 45' S	79° 06' W	NC	NC	¹⁴ C

*masl = meters above sea level; NC = Not Calculated

Upper Depth (cm)	Lower Depth (cm)	Age Years AD	K	Mn	Sr	Zn	Al	S	Ca	Na
Elemental Concentration ($\mu\text{g/g}$ dry sediment mass)										
46.5	47.0	1618	181	23	136	14	53	645	163721	127
48.5	49.0	1594	146	39	249	9	58	423	226947	216
50.5	51.0	1571	184	27	114	14	72	622	123519	96
52.5	53.0	1548	175	27	117	14	98	582	125093	99
54.5	55.0	1525	110	42	260	8	120	289	292075	107
56.5	57.0	1501	107	44	257	9	130	272	354516	74
58.5	59.0	1478	110	51	267	13	121	250	300445	73

Upper Depth (cm)	Lower Depth (cm)	Age Years AD	Fe	Pb	Ni	Ag	Cd	Sn	Sb	Tl
Elemental Concentrations ($\mu\text{g/g}$ dry sediment mass)										
0.5	1.0	2005	2156	114.01	17.35	0.279	0.489	0.208	0.532	0.460
2.5	3.0	2001	2088	122.97	15.22	0.233	0.662	0.182	0.476	0.433
4.5	5.0	1995	1430	170.49	28.49	0.484	0.448	0.369	0.949	0.744
6.5	7.0	1989	1389	167.28	16.07	0.265	0.976	0.226	0.596	0.485
8.5	9.0	1979	738	231.23	16.16	0.259	1.004	0.240	0.668	0.458
10.5	11.0	1972	596	311.07	15.86	0.249	1.400	0.257	0.815	0.571
12.5	13.0	1964	539	327.59	14.93	0.240	1.794	0.259	0.823	0.653
14.5	15.0	1955	367	416.60	15.00	0.234	2.107	0.300	0.977	0.652
16.5	17.0	1942	366	710.73	16.18	0.247	2.932	0.432	1.791	0.730
18.5	19.0	1932	385	429.05	15.87	0.245	1.799	0.335	1.312	0.555
20.5	21.0	1921	696	229.97	16.58	0.248	0.596	0.249	0.669	0.433
22.5	23.0	1905	314	87.78	16.40	0.256	0.044	0.198	0.551	0.398
24.5	25.0	1888	228	75.35	17.48	0.259	0.000	0.361	0.545	0.381
26.5	27.0	1850	224	60.43	15.63	0.235	0.000	0.180	0.405	0.343
28.5	29.0	1827	293	38.93	18.68	0.277	0.000	0.197	0.564	0.574
30.5	31.0	1804	66	17.85	15.53	0.226	0.000	0.159	0.302	0.301
32.5	33.0	1781								
34.5	35.0	1757	51	7.65	14.92	0.212	0.000	0.147	0.263	0.324
36.5	37.0	1734	22	4.13	15.55	0.223	0.000	0.148	0.251	0.323
38.5	39.0	1711	35	0.00	15.90	0.237	0.000	0.150	0.247	0.331
40.5	41.0	1688	25	0.00	15.77	0.221	0.000	0.142	0.238	0.314
42.5	43.0	1664	187	0.00	16.15	0.226	0.000	0.145	0.242	0.313
44.5	45.0	1641	49	0.00	15.16	0.212	0.000	0.145	0.237	0.283
46.5	47.0	1618	34	0.00	17.46	0.237	0.000	0.160	0.252	0.315
48.5	49.0	1594	31	0.00	18.44	0.246	0.000	0.158	0.260	0.315
50.5	51.0	1571	36	0.00	15.86	0.198	0.000	0.131	0.212	0.271
52.5	53.0	1548	35	0.00	16.05	0.204	0.000	0.138	0.219	0.281

Upper Depth (cm)	Lower Depth (cm)	Age Years AD	Fe	Pb	Ni	Ag	Cd	Sn	Sb	Tl
Elemental Concentrations ($\mu\text{g/g}$ dry sediment mass)										
54.5	55.0	1525	35	0.00	15.70	0.210	0.000	0.164	0.223	0.282
56.5	57.0	1501	43	0.00	13.94	0.177	0.000	0.115	0.190	0.252
58.5	59.0	1478	34	0.00	11.73	0.154	0.000	0.117	0.173	0.220

Upper Depth (cm)	Lower Depth (cm)	Age Years AD	V	Co	Cu	As	Bi	Ti
Elemental Concentration ($\mu\text{g/g}$ dry sediment mass)								
0.5	1.0	2005	8.542	0.472	12.976	14.037	0.301	1.590
2.5	3.0	2001	8.753	0.441	14.436	13.671	0.268	2.076
4.5	5.0	1995	7.868	0.526	20.497	19.479	0.376	2.505
6.5	7.0	1989	6.853	0.381	18.773	19.279	0.307	1.859
8.5	9.0	1979	4.387	0.343	25.687	27.923	0.238	1.097
10.5	11.0	1972	3.838	0.312	36.781	29.904	0.336	1.401
12.5	13.0	1964	4.185	0.277	42.845	32.142	0.422	1.019
14.5	15.0	1955	4.555	0.236	45.416	34.323	0.367	0.949
16.5	17.0	1942	6.031	0.214	70.201	68.277	0.670	0.773
18.5	19.0	1932	4.091	0.256	40.798	52.345	0.433	0.937
20.5	21.0	1921	3.087	0.242	17.975	36.479	0.144	0.926
22.5	23.0	1905	2.772	0.248	9.477	19.410	0.077	0.787
24.5	25.0	1888	2.930	0.233	10.051	19.343	0.738	0.579
26.5	27.0	1850	3.193	0.223	8.678	20.794	0.041	0.564
28.5	29.0	1827	2.547	0.293	8.837	17.699	0.138	1.276
30.5	31.0	1804	1.740	0.194	3.307	6.898	0.000	0.587
32.5	33.0	1781			Sample lost			
34.5	35.0	1757	2.238	0.150	1.729	6.876	0.000	0.375
36.5	37.0	1734	1.713	0.139	1.103	5.448	0.000	0.346
38.5	39.0	1711	2.093	0.140	1.305	5.357	0.000	0.364
40.5	41.0	1688	2.005	0.139	1.397	5.044	0.000	0.387
42.5	43.0	1664	2.729	0.153	1.573	5.988	0.000	0.372
44.5	45.0	1641	2.287	0.161	1.443	7.236	0.000	0.878
46.5	47.0	1618	3.112	0.179	1.861	6.541	0.000	0.473
48.5	49.0	1594	3.102	0.153	0.898	8.111	0.000	0.380
50.5	51.0	1571	2.645	0.144	1.254	8.460	0.000	0.433
52.5	53.0	1548	2.218	0.131	1.154	6.382	0.043	0.581
54.5	55.0	1525	1.993	0.130	0.635	4.267	0.000	0.384
56.5	57.0	1501	1.686	0.108	0.625	3.738	0.000	0.462
58.5	59.0	1478	1.878	0.103	0.584	4.773	0.136	0.341

**B.2 TABLES OF ELEMENTAL CONCENTRATION DATA FROM LAGUNA
PIRHUACOCHA**

Upper Depth (cm)	Lower Depth (cm)	Age Cal Yrs. AD	K	Mn	Sr	Zn	Al	S	Ca	Na
Elemental Concentration ($\mu\text{g/g}$ dry sediment)										
0.0	0.5	2005	199	34942	107	835	4143	5295	21215	94
0.5	1.0	2001	164	17337	71	810	4642	12985	17432	94
1.0	1.5	1996	180	9778	66	796	4642	21397	18133	88
1.5	2.0	1988	179	7004	61	672	5972	16324	15427	72
2.0	2.5	1981	183	5662	53	601	5067	15207	12750	67
2.5	3.0	1974	228	5063	53	599	5822	17191	13032	83
3.0	3.5	1967	315	3981	41	408	5456	13428	10332	47
3.5	4.0	1959	313	3923	46	314	5935	12762	10983	50
4.0	4.5	1951	184	3904	53	222	5710	12241	11973	61
4.5	5.0	1942	171	4117	54	179	6013	11163	12861	59
5.0	5.5	1934	159	4330	56	136	6316	10084	13748	57
5.5	6.0	1927	217	4751	67	115	7542	6933	19437	70
6.0	6.5	1920	175	3956	61	100	6686	6642	16446	68
6.5	7.0	1912	171	4004	56	101	7410	7542	12715	50
7.0	7.5	1904	168	3673	53	91	7454	7955	11947	47
7.5	8.0	1896	166	3342	50	80	7499	8369	11178	44
8.0	8.5	1889	153	3252	53	91	7520	14463	14527	58
8.5	9.0	1874	153	4156	52	76	7993	8040	12068	55
9.0	9.5	1858	135	5665	50	68	9100	6854	14333	53
9.5	10.0	1843	128	3749	44	69	6782	6133	10968	40
9.5	10.0	1843	139	3645	48	79	6774	7043	10605	44
10.0	10.5	1828	129	4944	50	78	6513	9808	11971	53
10.5	11.0	1813	144	6263	51	80	6741	8415	12125	48
11.0	11.5	1797	140	7960	53	81	6686	10903	12982	43
11.5	12.0	1782	164	6373	56	89	6714	14517	13886	54
12.0	12.5	1767	150	6052	55	80	6132	14080	13379	48
12.5	13.0	1752	135	5731	55	71	5551	13643	12873	42
13.0	13.5	1736	131	12568	53	73	5591	11442	13504	43
13.5	14.0	1721	124	29774	53	76	5395	8401	15225	39
14.0	14.5	1706	113	47673	57	64	4605	5122	17689	36
14.5	15.0	1691	121	40773	52	65	5166	5335	15229	40
15.0	15.5	1675	128	33873	47	66	5726	5549	12769	43
15.5	16.0	1660	123	27829	46	60	5418	4473	11499	38
16.0	16.5	1645	156	25711	52	70	7016	6628	11859	53
16.5	17.0	1630	144	17188	50	62	7662	5003	11836	61
17.0	17.5	1615	149	12866	52	55	9125	4187	14024	82
17.5	18.0	1599	155	8545	54	48	10589	3372	16212	102

Upper Depth (cm)	Lower Depth (cm)	Age Cal Yrs. AD	K	Mn	Sr	Zn	Al	S	Ca	Na
Elemental Concentration ($\mu\text{g/g}$ dry sediment)										
18.0	18.5	1584	170	9050	55	47	11062	2989	16060	95
18.5	19.0	1569	195	7455	57	48	12564	1519	15193	103
19.0	19.5	1554	208	7184	57	54	12391	1403	12412	86
19.5	20.0	1538	230	5788	61	53	12785	769	11963	85
19.5	20.0	1538	228	6098	61	53	12975	783	12546	88
20.0	20.5	1523	236	5287	60	55	12395	943	12473	88
20.5	21.0	1508	201	5613	54	46	12186	1105	12444	78
21.0	21.5	1493	188	6316	54	46	10924	1874	12236	72
21.5	22.0	1477	195	8158	56	50	78111	2508	16921	73
22.0	22.5	1462	211	6068	60	53	73076	2180	13794	99
22.5	23.0	1447	172	6935	52	46	71650	710	10941	79
23.0	23.5	1432	195	6368	60	53	82886	1216	13682	98
23.5	24.0	1416	212	6883	53	58	79799	1101	12278	80
24.0	24.5	1401	215	5761	54	55	79065	1326	12043	75
24.5	25.0	1386	225	4699	56	57	78017	1569	11413	105
25.0	25.5	1371	235	3638	58	58	76968	1812	10783	136
25.5	26.0	1355	224	3852	58	61	75345	1880	10462	117
26.0	26.5	1340	228	3978	64	57	68041	1853	10668	126
26.5	27.0	1325	208	3330	65	51	58550	1837	10798	117
27.0	27.5	1310	202	2631	78	49	54045	1605	11257	141
27.5	28.0	1295	197	1932	91	47	49541	1372	11717	165
28.0	28.5	1279	240	2736	59	53	62918	749	11911	125
28.5	29.0	1264	254	3871	59	59	64401	471	12402	119
29.0	29.5	1249	234	3801	58	54	64376	734	12270	121
29.5	30.0	1234	232	4552	57	56	62020	339	11942	110
30.0	30.5	1234	240	4602	57	56	62291	427	11993	117
30.5	31.0	1218	219	4418	55	55	61469	603	11049	112
31.0	31.5	1203	237	4199	52	53	55844	387	10958	115
31.5	32.0	1188	262	3013	56	59	44519	281	11767	120
32.0	32.5	1173	230	2942	56	59	52971	467	11552	115
32.5	33.0	1157	228	2426	55	52	46168	401	11776	115
33.0	33.5	1142	226	1910	55	45	39364	336	12000	115
33.5	34.0	1127	240	1906	58	46	41305	317	15400	139
34.0	34.5	1112	220	2085	56	46	39681	271	12587	124
34.5	35.0	1096	234	2461	59	52	40684	456	12681	117
35.0	35.5	1081	238	2509	61	54	40092	489	12955	120
35.5	36.0	1066	243	2558	63	55	39501	523	13228	122
36.0	36.5	1051	252	2633	62	55	46229	395	15317	122
36.5	37.0	1035	268	2124	69	57	41204	402	13988	128
37.0	37.5	1020	240	1960	69	57	41530	619	13211	127
37.5	38.0	1005	241	2207	68	59	43340	511	13971	133
38.0	38.5	990	243	2455	68	60	45150	404	14731	140
38.5	39.0	983	243	2545	69	59	43190	402	14043	133
39.0	39.5	972	263	2445	69	61	41106	375	13819	129
39.5	40.0	961	265	2425	71	66	39595	421	13677	136
40.0	40.5	950	235	2167	65	60	39535	404	12236	126
40.5	41.0	950	215	2140	61	55	38327	364	12013	121

Upper Depth (cm)	Lower Depth (cm)	Age Cal Yrs. AD	K	Mn	Sr	Zn	Al	S	Ca	Na
Elemental Concentration ($\mu\text{g/g}$ dry sediment)										
41.0	41.5	939	270	2566	68	73	39488	355	13678	131
41.5	42.0	928	252	2689	70	77	41197	451	12764	129
42.0	42.5	917	260	3344	71	83	17210	446	14327	127
42.5	43.0	907	242	3689	67	77	16190	461	14131	121
43.0	43.5	896	246	3964	66	74	18175	414	14944	122
43.5	44.0	885	249	4240	65	71	20161	368	15758	122
44.0	44.5	874	267	3440	65	75	18070	355	12866	121
44.5	45.0	863	216	3945	65	67	17996	227	13860	120
45.0	45.5	852	201	3665	64	61	16507	220	12832	114
45.5	46.0	841	205	3564	65	64	15218	329	12973	119
46.0	46.5	830	209	3462	67	67	13930	438	13113	124
46.5	47.0	819	243	3462	68	71	13930	189	13113	117
47.0	47.5	808	230	4560	68	75	18005	374	16636	119
47.5	48.0	797	384	4388	70	76	16507	268	16320	451
48.0	48.5	786	300	4634	67	74	16263	280	16256	288
48.5	49.0	775	216	4880	64	71	16019	293	16193	125
49.0	49.5	764	205	5476	60	69	14382	289	14524	115
49.5	50.0	753	194	5104	60	65	12911	498	14263	120
50.0	50.5	742	168	5982	59	60	13401	1810	16229	118
50.5	51.0	731	147	6340	61	53	11547	1036	17132	120
51.0	51.5	731	139	6013	59	52	11109	977	15715	116
51.5	52.0	720	142	7769	62	50	10124	3286	15735	121
52.0	52.5	710	143	9239	64	49	10726	3833	20280	125
52.5	53.0	699	134	10366	64	43	9817	6029	22470	119
53.0	53.5	688	143	12912	69	45	9690	7492	23419	123
53.5	54.0	677	135	22351	68	44	9903	5170	22567	117
54.0	54.5	666	128	31790	66	44	10116	2848	21714	111
54.5	55.0	655	126	34228	58	44	8292	1503	16789	106
55.0	55.5	644	130	24395	53	46	8766	2335	13899	106
55.5	56.0	633	131	18512	52	47	9142	4470	12867	111
56.0	56.5	622	129	18055	53	44	9654	3656	13788	110
56.5	57.0	611	127	17597	54	42	10166	2842	14709	109
57.0	57.5	600	130	13201	58	40	8527	2888	14384	114
57.5	58.0	589	131	9418	56	40	8198	2380	12611	108
58.0	58.5	578	144	5646	58	42	8880	3216	13174	112
58.5	59.0	567	157	4540	59	40	9974	2485	14255	112
59.0	59.5	556	171	3434	60	39	11068	1754	15337	112
59.5	60.0	545	161	3845	58	37	11759	1284	17607	108
60.0	60.5	534	181	3523	59	39	10507	792	15243	114
60.5	61.0	523	172	3756	56	37	10692	1033	14297	109
61.0	61.5	513	158	3980	54	35	10145	491	15012	108
61.5	62.0	513	160	4051	55	36	10574	475	15169	109
62.0	62.5	458	111	7071	37	31	7890	364	12340	73
62.5	63.0	403	115	3849	39	42	8480	999	10104	74
63.0	63.5	348	177	2672	47	44	13596	473	11835	91
63.5	64.0	294	205	2582	50	45	11751	476	13288	88
64.0	64.5	239	140	3427	42	45	7928	1300	16470	79

Upper Depth (cm)	Lower Depth (cm)	Age Cal Yrs. AD	K	Mn	Sr	Zn	Al	S	Ca	Na
Elemental Concentration ($\mu\text{g/g}$ dry sediment)										
64.5	65.0	184	111	2100	37	43	7321	1215	15600	76
65.0	65.5	130	83	2895	36	30	4728	2165	22361	68
65.5	66.0	75	162	2599	53	50	9945	816	19745	112
66.0	66.5	20	145	2257	46	53	9144	797	13159	92
66.5	67.0	-35	172	2220	58	47	12089	1097	15074	119
67.0	67.5	-89	148	1630	48	48	9323	1070	14742	94

Upper Depth (cm)	Lower Depth (cm)	Age Cal Yrs. AD	Fe	Ti	Pb	Co	Ni	Cu	V
Elemental Concentration ($\mu\text{g/g}$ dry sediment)									
0.0	0.5	2005	168802	42	1401	28	37	146	15
0.5	1.0	2001	138882	45	1493	25	34	142	21
1.0	1.5	1996	125000	48	1593	29	40	153	31
1.5	2.0	1988	116081	49	1882	27	41	147	32
2.0	2.5	1981	110160	42	2260	28	33	142	27
2.5	3.0	1974	129110	44	2512	30	39	170	32
3.0	3.5	1967	106434	31	1446	30	36	102	25
3.5	4.0	1959	109414	34	1016	34	41	69	31
4.0	4.5	1951	119955	45	608	32	39	53	38
4.5	5.0	1942	118560	48	414	32	41	45	37
5.0	5.5	1934	117164	51	220	32	42	37	35
5.5	6.0	1927	127882	56	157	35	47	36	35
6.0	6.5	1920	119130	49	122	30	43	34	38
6.5	7.0	1912	126901	56	115	31	47	32	39
7.0	7.5	1904	119624	52	99	31	47	32	38
7.5	8.0	1896	112347	47	82	30	46	32	37
8.0	8.5	1889	131793	57	102	35	47	33	37
8.5	9.0	1874	118175	59	88	29	44	27	38
9.0	9.5	1858	124792	51	83	30	40	26	34
9.5	10.0	1843	131302	51	93	27	33	24	31
9.5	10.0	1843	124286	59	103	30	39	28	34
10.0	10.5	1828	133940	60	91	29	38	27	34
10.5	11.0	1813	125153	64	115	29	37	26	34
11.0	11.5	1797	127844	73	111	33	41	30	38
11.5	12.0	1782	110036	87	123	31	46	34	41
12.0	12.5	1767	102684	87	102	32	45	31	44
12.5	13.0	1752	95332	86	82	33	44	29	46
13.0	13.5	1736	113898	74	103	42	41	27	39
13.5	14.0	1721	128002	64	108	35	36	22	29
14.0	14.5	1706	139616	54	82	33	30	20	18
14.5	15.0	1691	140829	58	81	32	33	21	24
15.0	15.5	1675	142042	61	80	30	35	22	31
15.5	16.0	1660	133817	55	80	28	34	15	26
16.0	16.5	1645	136201	65	75	35	44	22	35
16.5	17.0	1630	119317	54	60	34	44	21	37
17.0	17.5	1615	109012	51	47	34	47	23	39

Upper Depth (cm)	Lower Depth (cm)	Age Cal Yrs. AD	Fe	Ti	Pb	Co	Ni	Cu	V
Elemental Concentration (µg/g dry sediment)									
17.5	18.0	1599	98707	48	35	34	49	24	40
18.0	18.5	1584	83387	46	31	39	57	31	47
18.5	19.0	1569	78083	42	25	42	62	28	48
19.0	19.5	1554	72523	36	34	49	60	39	48
19.5	20.0	1538	65118	34	28	50	63	43	51
19.5	20.0	1538	68771	34	33	45	63	42	47
20.0	20.5	1523	60757	38	31	49	63	43	50
20.5	21.0	1508	65887	39	30	40	54	34	41
21.0	21.5	1493	65505	41	30	41	52	31	46
21.5	22.0	1477	16616	46	30	39	56	34	45
22.0	22.5	1462	16696	48	39	39	59	34	47
22.5	23.0	1447	11606	41	27	40	51	28	51
23.0	23.5	1432	16295	42	28	45	64	37	55
23.5	24.0	1416	12511	37	36	45	54	38	56
24.0	24.5	1401	13978	39	29	45	55	36	52
24.5	25.0	1386	14203	42	35	43	58	35	52
25.0	25.5	1371	14427	44	41	41	60	33	52
25.5	26.0	1355	14659	46	48	41	59	31	56
26.0	26.5	1340	16776	50	48	40	62	34	49
26.5	27.0	1325	19617	51	43	33	59	31	55
27.0	27.5	1310	23081	48	36	38	69	28	48
27.5	28.0	1295	26546	45	29	43	80	26	41
28.0	28.5	1279	17245	41	24	46	66	38	56
28.5	29.0	1264	15334	43	31	43	65	39	58
29.0	29.5	1249	15011	43	30	46	63	40	58
29.5	30.0	1234	15453	36	28	43	58	40	56
30.0	30.5	1234	15632	38	29	42	61	40	56
30.5	31.0	1218	13511	39	36	40	56	40	54
31.0	31.5	1203	13644	35	25	39	55	40	54
31.5	32.0	1188	13512	31	21	41	57	45	57
32.0	32.5	1173	12471	30	32	40	54	44	56
32.5	33.0	1157	13499	35	26	39	58	41	57
33.0	33.5	1142	14527	39	20	38	61	37	58
33.5	34.0	1127	15997	37	16	41	68	35	47
34.0	34.5	1112	14415	39	18	40	68	34	44
34.5	35.0	1096	13828	38	22	41	61	41	50
35.0	35.5	1081	14264	42	22	45	65	44	53
35.5	36.0	1066	14700	46	23	48	68	46	55
36.0	36.5	1051	15829	48	19	47	67	46	54
36.5	37.0	1035	16876	44	19	42	65	50	57
37.0	37.5	1020	16308	37	16	48	68	50	55
37.5	38.0	1005	17017	36	16	46	64	50	55
38.0	38.5	990	17725	35	17	44	61	51	55
38.5	39.0	983	17672	40	15	46	60	52	58
39.0	39.5	972	16554	39	15	45	65	52	60
39.5	40.0	961	14901	46	17	48	68	53	62
40.0	40.5	950	13041	44	17	45	67	46	57

Upper Depth (cm)	Lower Depth (cm)	Age Cal Yrs. AD	Fe	Ti	Pb	Co	Ni	Cu	V
			Elemental Concentration (µg/g dry sediment)						
40.5	41.0	950	13055	42	16	43	60	43	52
41.0	41.5	939	13726	46	21	47	68	51	60
41.5	42.0	928	12808	45	18	48	69	55	65
42.0	42.5	917	52632	47	22	50	73	55	68
42.5	43.0	907	53663	47	20	49	72	51	64
43.0	43.5	896	59241	50	20	48	72	48	63
43.5	44.0	885	64819	53	20	47	72	46	62
44.0	44.5	874	55829	53	23	48	74	47	66
44.5	45.0	863	62690	42	23	46	66	46	63
45.0	45.5	852	60825	38	19	44	60	41	62
45.5	46.0	841	54317	37	18	45	62	44	64
46.0	46.5	830	51063	37	18	45	63	48	67
46.5	47.0	819	47808	33	19	44	63	44	69
47.0	47.5	808	67595	37	19	42	62	49	67
47.5	48.0	797	60366	37	18	43	63	44	67
48.0	48.5	786	63263	38	18	44	68	42	65
48.5	49.0	775	66160	39	18	45	73	40	63
49.0	49.5	764	58910	36	18	37	60	32	56
49.5	50.0	753	63009	42	17	43	65	30	60
50.0	50.5	742	88889	47	16	42	65	31	56
50.5	51.0	731	91721	51	16	39	59	34	52
51.0	51.5	731	88039	48	15	37	56	30	50
51.5	52.0	720	85699	54	15	36	55	33	50
52.0	52.5	710	84380	54	15	40	56	31	44
52.5	53.0	699	96957	58	13	40	53	32	46
53.0	53.5	688	105097	66	14	46	56	30	48
53.5	54.0	677	112776	60	15	44	54	30	47
54.0	54.5	666	120455	54	16	43	52	29	45
54.5	55.0	655	115280	61	18	34	45	23	34
55.0	55.5	644	122181	58	17	34	49	22	29
55.5	56.0	633	120350	57	16	37	54	24	34
56.0	56.5	622	124769	49	16	36	52	23	35
56.5	57.0	611	129188	42	16	35	50	22	37
57.0	57.5	600	111159	42	17	37	52	25	40
57.5	58.0	589	100512	37	14	37	51	28	44
58.0	58.5	578	85242	39	14	37	53	32	47
58.5	59.0	567	77574	41	14	39	55	33	47
59.0	59.5	556	69905	43	13	41	57	34	46
59.5	60.0	545	71972	40	13	40	53	31	38
60.0	60.5	534	49198	43	13	39	54	31	44
60.5	61.0	523	61670	42	14	37	53	35	41
61.0	61.5	513	61009	39	13	35	51	29	37
61.5	62.0	513	62724	39	13	36	52	30	36
62.0	62.5	458	59920	43	11	26	43	13	26
62.5	63.0	403	65915	49	15	29	43	15	37
63.0	63.5	348	51013	52	15	37	60	27	42
63.5	64.0	294	41284	60	15	37	61	28	44

Upper Depth (cm)	Lower Depth (cm)	Age Cal Yrs. AD	Fe	Ti	Pb	Co	Ni	Cu	V
Elemental Concentration (µg/g dry sediment)									
64.0	64.5	239	42321	44	13	31	48	25	39
64.5	65.0	184	44856	44	12	24	41	22	32
65.0	65.5	130	28005	35	10	19	34	17	28
65.5	66.0	75	42084	48	15	37	62	27	38
66.0	66.5	20	44461	48	14	34	57	28	43
66.5	67.0	-35	43075	47	15	38	63	35	45
67.0	67.5	-89	33933	37	12	31	54	32	38

Upper Depth (cm)	Lower Depth (cm)	Age Cal Yrs. AD	Ag	Cd	Sn	Sb	Bi	As
Elemental Concentration (µg/g dry sediment)								
0.0	0.5	2005	1.5	26.7	3.4	13.8	53.2	1116.4
0.5	1.0	2001	0.1	18.6	3.3	10.0	35.3	606.7
1.0	1.5	1996	0.6	17.5	2.9	8.3	34.8	357.7
1.5	2.0	1988	0.9	16.9	3.3	8.4	48.8	282.8
2.0	2.5	1981	0.0	15.2	4.4	6.7	56.9	273.5
2.5	3.0	1974	0.9	12.9	4.9	7.8	72.4	227.6
3.0	3.5	1967	0.5	8.4	2.8	4.4	39.3	153.8
3.5	4.0	1959	0.0	6.2	1.9	2.9	18.0	127.1
4.0	4.5	1951	0.2	4.3	1.3	2.5	11.0	135.4
4.5	5.0	1942	0.1	3.0	0.9	1.6	6.9	114.1
5.0	5.5	1934	0.0	1.8	0.5	0.7	2.9	92.8
5.5	6.0	1927	0.0	1.4	0.3	0.7	2.3	78.2
6.0	6.5	1920	0.0	1.2	0.3	0.5	1.8	55.8
6.5	7.0	1912	0.0	1.3	0.3	0.5	2.0	57.9
7.0	7.5	1904	0.0	1.1	0.3	0.4	1.7	49.0
7.5	8.0	1896	0.0	0.9	0.2	0.3	1.4	40.2
8.0	8.5	1889	0.1	1.1	0.3	0.5	2.1	47.6
8.5	9.0	1874	0.0	0.9	0.2	0.3	1.5	38.1
9.0	9.5	1858	0.1	0.9	0.3	0.4	1.9	37.1
9.5	10.0	1843	0.0	1.0	0.3	0.4	1.8	44.4
9.5	10.0	1843	0.0	1.0	0.3	0.4	1.8	43.2
10.0	10.5	1828	0.0	0.9	0.3	0.3	1.4	43.1
10.5	11.0	1813	0.0	1.1	0.3	0.5	2.0	47.5
11.0	11.5	1797	0.0	1.1	0.3	0.4	1.8	39.8
11.5	12.0	1782	0.0	1.3	0.4	0.6	2.4	46.5
12.0	12.5	1767	0.0	1.2	0.3	0.5	1.8	44.0
12.5	13.0	1752	0.1	1.1	0.2	0.5	1.2	41.4
13.0	13.5	1736	0.0	1.2	0.3	0.6	1.8	50.2
13.5	14.0	1721	0.1	1.2	0.3	0.7	2.3	56.1
14.0	14.5	1706	0.0	0.9	0.3	0.4	1.6	44.0
14.5	15.0	1691	0.0	0.9	0.4	0.4	1.5	39.2
15.0	15.5	1675	0.0	0.9	0.4	0.4	1.3	34.5
15.5	16.0	1660	0.1	0.8	0.4	0.4	1.2	32.0
16.0	16.5	1645	0.0	0.9	0.3	0.4	1.5	32.1
16.5	17.0	1630	0.0	0.7	0.2	0.2	0.8	22.6

Upper Depth (cm)	Lower Depth (cm)	Age Cal Yrs. AD	Ag	Cd	Sn	Sb	Bi	As
Elemental Concentration (µg/g dry sediment)								
17.0	17.5	1615	0.0	0.5	0.2	0.2	0.7	17.3
17.5	18.0	1599	0.0	0.4	0.1	0.1	0.5	12.0
18.0	18.5	1584	0.0	0.3	0.1	0.1	0.4	8.4
18.5	19.0	1569	0.0	0.3	0.1	0.1	0.3	4.5
19.0	19.5	1554	0.0	0.3	0.1	0.1	0.4	4.7
19.5	20.0	1538	0.0	0.3	0.1	0.0	0.2	3.1
19.5	20.0	1538	0.0	0.3	0.1	0.0	0.3	3.3
20.0	20.5	1523	0.0	0.3	0.1	0.0	0.3	3.3
20.5	21.0	1508	0.0	0.3	0.1	0.1	0.4	3.9
21.0	21.5	1493	0.0	0.3	0.1	0.1	0.3	4.6
21.5	22.0	1477	0.1	0.3	0.1	0.1	0.4	6.6
22.0	22.5	1462	0.0	0.3	0.1	0.1	0.5	6.0
22.5	23.0	1447	0.0	0.2	0.1	0.0	0.2	3.5
23.0	23.5	1432	0.0	0.2	0.1	0.0	0.3	3.5
23.5	24.0	1416	0.0	0.3	0.1	0.1	0.3	3.8
24.0	24.5	1401	0.1	0.2	0.1	0.0	0.3	3.2
24.5	25.0	1386	0.1	0.3	0.1	0.1	0.4	4.2
25.0	25.5	1371	0.1	0.3	0.1	0.1	0.5	5.2
25.5	26.0	1355	0.0	0.4	0.1	0.1	0.6	5.5
26.0	26.5	1340	0.0	0.4	0.1	0.1	0.6	5.3
26.5	27.0	1325	0.1	0.4	0.2	0.1	0.6	5.1
27.0	27.5	1310	0.1	0.3	0.1	0.1	0.5	4.4
27.5	28.0	1295	0.1	0.2	0.1	0.1	0.4	3.8
28.0	28.5	1279	0.0	0.1	0.1	0.0	0.0	1.3
28.5	29.0	1264	0.0	0.2	0.1	0.0	0.1	1.6
29.0	29.5	1249	0.1	0.2	0.1	0.0	0.2	2.2
29.5	30.0	1234	0.0	0.2	0.1	0.0	0.1	1.5
30.0	30.5	1234	0.0	0.2	0.1	0.0	0.2	1.7
30.5	31.0	1218	0.0	0.3	0.1	0.1	0.3	2.1
31.0	31.5	1203	0.0	0.2	0.0	0.0	0.1	1.3
31.5	32.0	1188	0.0	0.1	0.0	0.0	0.1	0.9
32.0	32.5	1173	0.1	0.3	0.1	0.0	0.3	2.4
32.5	33.0	1157	0.0	0.2	0.1	0.0	0.2	1.7
33.0	33.5	1142	0.0	0.1	0.0	0.0	0.1	0.9
33.5	34.0	1127	0.0	0.1	0.0	0.0	0.0	0.8
34.0	34.5	1112	0.0	0.1	0.0	0.0	0.1	0.7
34.5	35.0	1096	0.0	0.1	0.0	0.0	0.0	0.8
35.0	35.5	1081	0.0	0.1	0.0	0.0	0.0	0.7
35.5	36.0	1066	0.0	0.1	0.0	0.0	0.0	0.7
36.0	36.5	1051	0.1	0.1	0.0	0.0	0.0	0.7
36.5	37.0	1035	0.0	0.2	0.0	0.0	0.0	0.6
37.0	37.5	1020	0.0	0.1	0.0	0.0	0.0	0.9
37.5	38.0	1005	0.0	0.2	0.0	0.0	0.0	0.8
38.0	38.5	990	0.0	0.2	0.0	0.0	0.0	0.7
38.5	39.0	983	0.0	0.2	0.0	0.0	0.0	0.8
39.0	39.5	972	0.0	0.2	0.0	0.0	0.0	0.6
39.5	40.0	961	0.0	0.2	0.0	0.0	0.0	0.8

Upper Depth (cm)	Lower Depth (cm)	Age Cal Yrs. AD	Ag	Cd	Sn	Sb	Bi	As
Elemental Concentration (µg/g dry sediment)								
40.0	40.5	950	0.0	0.2	0.0	0.0	0.0	0.8
40.5	41.0	950	0.0	0.2	0.0	0.0	0.0	0.9
41.0	41.5	939	0.0	0.2	0.0	0.0	0.0	0.7
41.5	42.0	928	0.0	0.3	0.0	0.0	0.0	0.7
42.0	42.5	917	0.2	0.3	0.0	0.0	0.0	1.0
42.5	43.0	907	0.0	0.3	0.1	0.0	0.0	0.9
43.0	43.5	896	0.0	0.3	0.0	0.0	0.0	0.9
43.5	44.0	885	0.0	0.3	0.0	0.0	0.0	0.9
44.0	44.5	874	0.0	0.3	0.0	0.0	0.0	0.6
44.5	45.0	863	0.0	0.3	0.0	0.0	0.0	0.7
45.0	45.5	852	0.0	0.3	0.1	0.0	0.0	0.7
45.5	46.0	841	0	0	0	0	0	0.8
46.0	46.5	830	0.0	0.3	0.1	0.0	0.0	0.9
46.5	47.0	819	0.0	0.3	0.0	0.0	0.0	0.7
47.0	47.5	808	0.1	0.3	0.1	0.0	0.0	0.8
47.5	48.0	797	0.0	0.3	0.1	0.0	0.0	0.8
48.0	48.5	786	0.0	0.3	0.1	0.0	0.0	0.8
48.5	49.0	775	0.0	0.3	0.1	0.0	0.0	0.9
49.0	49.5	764	0.1	0.2	0.0	0.0	0.0	0.7
49.5	50.0	753	0.0	0.2	0.1	0.0	0.0	0.8
50.0	50.5	742	0.0	0.2	0.1	0.0	0.0	1.4
50.5	51.0	731	0.0	0.2	0.1	0.0	0.0	1.9
51.0	51.5	731	0.1	0.2	0.1	0.0	0.0	2.1
51.5	52.0	720	0.9	0.2	0.1	0.0	0.0	2.7
52.0	52.5	710	0.0	0.2	0.1	0.0	0.0	3.8
52.5	53.0	699	0.0	0.2	0.1	0.0	0.0	5.5
53.0	53.5	688	0.0	0.2	0.1	0.0	0.0	7.3
53.5	54.0	677	0.0	0.2	0.1	0.0	0.0	6.0
54.0	54.5	666	0.0	0.2	0.1	0.0	0.0	4.7
54.5	55.0	655	0.0	0.1	0.1	0.0	0.0	3.0
55.0	55.5	644	0.0	0.1	0.1	0.0	0.0	3.0
55.5	56.0	633	0.0	0.2	0.1	0.0	0.0	4.1
56.0	56.5	622	0.0	0.1	0.1	0.0	0.0	3.5
56.5	57.0	611	0.0	0.1	0.1	0.0	0.0	2.8
57.0	57.5	600	0.1	0.1	0.0	0.0	0.0	3.3
57.5	58.0	589	0.0	0.1	0.0	0.0	0.0	2.3
58.0	58.5	578	0.0	0.1	0.0	0.0	0.0	2.2
58.5	59.0	567	0.0	0.1	0.1	0.0	0.0	1.7
59.0	59.5	556	0.0	0.1	0.1	0.0	0.0	1.2
59.5	60.0	545	0.0	0.1	0.1	0.0	0.0	1.2
60.0	60.5	534	0.0	0.1	0.1	0.0	0.0	0.8
60.5	61.0	523	0.0	0.1	0.1	0.0	0.0	0.9
61.0	61.5	513	0.0	0.1	0.1	0.0	0.0	1.1
61.5	62.0	513	0.0	0.1	0.1	0.0	0.0	0.9
62.0	62.5	458	0.0	0.1	0.1	0.0	0.0	1.6
62.5	63.0	403	0.0	0.2	0.1	0.0	0.0	1.8
63.0	63.5	348	0.0	0.2	0.1	0.0	0.0	0.6

Upper Depth (cm)	Lower Depth (cm)	Age Cal Yrs. AD	Ag	Cd	Sn	Sb	Bi	As
Elemental Concentration (µg/g dry sediment)								
63.5	64.0	294	0.0	0.2	0.1	0.0	0.0	0.7
64.0	64.5	239	0.0	0.3	0.1	0.0	0.0	1.6
64.5	65.0	184	0.0	0.2	0.1	0.0	0.0	2.1
65.0	65.5	130	0.0	0.2	0.1	0.0	0.0	7.3
65.5	66.0	75	0.0	0.2	0.1	0.0	0.0	1.2
66.0	66.5	20	0.0	0.3	0.1	0.0	0.0	1.0
66.5	67.0	-35	0.0	0.2	0.1	0.0	0.0	1.0
67.0	67.5	-89	0.0	0.2	0.1	0.0	0.0	1.1

B.3 TABLE OF LEAD CONCENTRATION DATA FROM LTCK

Depth Range (cm)	Year BC-AD	Pb $\mu\text{g g}^{-1}$
1-2 cm	1923	10
2-3 cm	1877	14
3-4 cm	1830	13
4-5 cm	1784	17
5-6 cm	1737	11
6-7 cm	1691	15
7-8 cm	1644	11
8-9 cm	1598	18
9-10 cm	1551	13
10-11 cm	1504	22
11-12 cm	1458	21
12-13 cm	1411	18
13-14 cm	1365	13
14-15 cm	1318	13
15-16 cm	1272	11
16-17 cm	1225	7
17-18 cm	1179	9
18-19 cm	1132	16
19-20 cm	1086	22
20-21 cm	1039	24
21-22 cm	993	21
22-23 cm	946	23
23-24 cm	900	13
24-25 cm	853	22
25-26 cm	807	17
26-27 cm	760	16
27-28 cm	714	13
28-29 cm	667	12
29-30 cm	621	10
30-31 cm	574	19
31-32 cm	527	10
32-33 cm	479	11
33-34 cm	432	20
34-35 cm	384	6
35-36 cm	337	4
36-37 cm	289	6
37-38 cm	242	4
38-39 cm	194	5
39-40 cm	147	4
40-41cm	99	5
41-42 cm	52	4

Depth Range (cm)	Year BC-AD	Pb $\mu\text{g g}^{-1}$
42-43cm	4	4
43-44 cm	-43	2
44-45cm	-91	5
45-46 cm	-138	3
46-47cm	-186	6
47-48 cm	-233	3
48-49cm	-281	5
49-50 cm	-328	3
50-51cm	-575	23
53-54cm	-1161	23
55-56 cm	-1345	22
57-58 cm	-1529	23
59-60 cm	-1714	17
61-62 cm	-1898	20
63-64 cm	-2082	20
65-66 cm	-2221	17
67-68 cm	-2359	16
69-70 cm	-2498	15
71-72 cm	-2636	14
73-74 cm	-2775	10
75-76 cm	-2914	14
77-78 cm	-3052	14
79-80 cm	-3191	10
81-82 cm	-3330	9
83-84 cm	-3468	14
85-86 cm	-3607	11
87-88 cm	-3745	8
89-90 cm	-3884	13
91-92 cm	-3944	5
93-94 cm	-4003	8
95-96 cm	-4063	12
97-98 cm	-4122	13
99-100 cm	-4182	17
101-102 cm	-4241	17

BIBLIOGRAPHY

- Abbott, M. B., Binford, M. W., Brenner, M., and Kelts, K. R. (1997a). A 350014C yr High-Resolution Record of Water-Level Changes in Lake Titicaca, Bolivia/Peru. *Quaternary Research* **47**, 169-180.
- Abbott, M. B., Seltzer, G. O., Kelts, K. R., and Southon, J. (1997b). Holocene Paleohydrology of the Tropical Andes from Lake Records. *Quaternary Research* **47**, 70-80.
- Abbott, M. B., and Wolfe, A. P. (2003). Intensive Pre-Incan Metallurgy Recorded by Lake Sediments from the Bolivian Andes. *Science* **301**, 1893-1895.
- Abbott, M. B., Wolfe, B. B., Aravena, R., Wolfe, A. P., and Seltzer, G. O. (2000). Holocene hydrological reconstructions from stable isotopes and paleolimnology, Cordillera Real, Bolivia. *Quaternary Science Reviews* **19**, 1801-1820.
- Appleby, P. G. (2001). Chronostratigraphic techniques in recent sediments. In "Tracking Environmental Changes Using Lake Sediments." (W. Last, M., and J. Smol, P., Eds.), pp. 171-203.
- Bakewell, P. (1984). "Miners of the Red Mountain: Indian Labor at Potosi, 1545-1650." University of New Mexico Press, Albuquerque.
- Baron, S., Lavoie, M., Ploquin, A., Carignan, J., Pulido, M., and deBeaulieu, J. L. (2005). Record of Metal Workshops in Peat Deposits: History and Environmental Impact on the Mont Lozère Massif, France. *Environmental Science and Technology* **39**, 5131-5140.
- Bauer, B., and Stanish, C. (2001). "Ritual and Pilgrimage in the Ancient Andes: The Islands of the Sun and the Moon." University of Austin, Austin, TX.
- Benavides Q., A. (1990). Exploration and mining ventures in Peru. *Economic Geology* **85**, 1296-1302.
- Bindler, R., Renberg, I., John Anderson, N., Appleby, P. G., Emteryd, O., and Boyle, J. (2001). Pb isotope ratios of lake sediments in West Greenland: inferences on pollution sources. *Atmospheric Environment* **35**, 4675-4685.
- Binford, M. W. (1990). Calculation and uncertainty analysis of ²¹⁰Pb dates for PIRLA project lake sediment cores. *Journal of Paleolimnology* **3**, 253-267.
- Binford, M. W., Kolata, A. L., Brenner, M., Janusek, J. W., Seddon, M. T., Abbott, M., and Curtis, J. H. (1997). Climate Variation and the Rise and Fall of an Andean Civilization. *Quaternary Research* **47**, 235-248.
- Blomqvist, S. (1991). Quantitative sampling of soft-bottom sediments: problems and solutions. *Mar. Ecol. Prog. Ser.* **72**, 295-304.
- Boutron, C. F., Gorlack, U., Candelone, J.-P., Bolshov, M. A., and Delmas, R. J. (1991). Decrease in anthropogenic lead, cadmium and zinc in Greenland snows since the late 1960s. *Nature* **353**, 153-156.

- Boyle, J. F. (2001). Inorganic geochemical methods in paleolimnology. In "Tracking Environmental Change Using Lake Sediments." (W. M. L. J. P. Smol, Ed.), pp. 83-141. Kluwer Academic Publishers, Dordrecht, The Netherlands.
- Brännvall, M.-L., Kurkkio, H., Bindler, R., Emteryd, O., and Renberg, I. (2001). The role of pollution versus natural geological sources for lead enrichment in recent lake sediments and surface forest soils. *Environmental Geology* **40**, 1057-1065.
- Callaway, M. (2005). Ice-cores, sediments and civilisation collapse: a cautionary tale from Lake Titicaca. *Antiquity* **79**, 778-790.
- Carignan, J., Simonetti, A., and Gariépy, C. (2002). Dispersal of atmospheric lead in northeastern North America as recorded by epiphytic lichens. *Atmospheric Environment* **36**, 3759-3766.
- Cooke, C. (Chapter 2).
- Costin, C., Earle, T., Owen, B., and Russell, G. (1989). The Impact of Inca Conquest on Local Technology in the Upper Mantaro Valley, Perú. In "What's New? A Closer Look at the Process of Innovation." (S. E. van der Leeuw, and R. Torrence, Eds.), pp. 107-139. Unwin Hyman, London.
- Craig, A. K. (1989). In "Precious Metals, Coinage, and the Changes in Monetary Structures in Latin America, Europe, and Asia." (E. van Cauwenberghe, Ed.), pp. 159-183. Leuven University Press, Leuven, Netherlands.
- D'Altroy, T. N., and Hastorf, C. A. (1984). The distribution and contents of Inca state storehouses in the Xauxa region of Peru. *American Antiquity* **49**, 334-349.
- Dickin, A. P. (1995). "Radiogenic isotope geology." Cambridge University Press, Cambridge.
- Donahue, W., Allen, E., and Schindler, D. (2006). Impacts of Coal-Fired Power Plants on Trace Metals and Polycyclic Aromatic Hydrocarbons (PAHs) in Lake Sediments in Central Alberta, Canada. *Journal of Paleolimnology* **35**, 111-128.
- Doucet, C., and Carignan, J. (2001). Atmospheric Pb isotopic composition and trace metal concentration as revealed by epiphytic lichens: an investigation related to two altitudinal sections in Eastern France. *Atmospheric Environment* **35**, 3681-3690.
- Earle, T., D'Altroy, T., LeBlanc, C., Hastorf, C. A., and Levine, T. (1980). Changing settlement patterns in the Yanamarca valley, Peru. *Journal of New World Archaeology* **4**, 1-49.
- Einaudi, M. T. (1977). Environment of ore deposition at Cerro de Pasco, Peru. *Economic Geology* **72**, 893-924.
- Espi, E., Boutron, C. F., Hong, S., Pourchet, M., Ferrari, C., Shotyk, W., and Charlet, L. (1997). Changing Concentrations of Cu, Zn, Cd and Pb in a High Altitude Peat Bog from Bolivia during the Past Three Centuries. *Water, Air, & Soil Pollution* **100**, 289-296.
- Fisher, J. R. (1977). "Silver Mines and Silver Miners in Colonial Peru, 1776-1824." Centre for Latin American Studies, University of Liverpool, Liverpool.
- Gallon, C., Tessier, A., Gobeil, C., and Alfaro-De La Torre, M. C. (2004). Modeling diagenesis of lead in sediments of a Canadian Shield lake. *Geochimica et Cosmochimica Acta* **69**, 3531-3545.
- Gallon, C., Tessier, A., Gobeil, C., and Carignan, R. (2006). Historical Perspective of Industrial Lead Emissions to the Atmosphere from a Canadian Smelter. *Environ. Sci. Technol.* **40**, 741-747.
- Gordon, R., and Knopf, R. (2006). Metallurgy of Bronze used in Tools from Machu Picchu, Peru. *Archaeometry* **48**, 57-76.

- Gordon, R. B., and Rutledge, J. W. (1984). Bismuth Bronze from Machu Picchu, Peru. *Science* **233**, 585-586.
- Graney, J. R., Halliday, A. N., Keeler, G. J., Nriagu, J. O., Robbins, J. A., and Norton, S. A. (1995). Isotopic record of lead pollution in lake sediments from the northeastern United States. *Geochimica et Cosmochimica Acta* **59**, 1715-1728.
- Gunnesch, K. A., Baumann, A., and Gunnesch, M. (1990). Lead Isotope Variations across the Central Peruvian Andes. *Economic Geology* **85**, 1384-1401.
- Hamelin, B., Grousset, F., and Sholkovitz, E. R. (1990). Pb isotopes in surficial pelagic sediments from the North Atlantic *Geochimica et Cosmochimica Acta* **54**, 37-47.
- Hastorf, C. A. (1990). The effect of the Inka state on Sausa agricultural production and crop consumption. *American Antiquity* **55**, 262-290.
- Hastorf, C. A., Earle, T., Wright, H. E., LeCount, L., Russell, G., and Sandefur, E. (1989). Settlement Archaeology in the Jauja Region of Peru: Evidence from the Early Intermediate Period through the Late Horizon: A Report on the 1986 Field Season. *Andean Past* **2**, 81-129.
- Hong, S., Candelone, J.-P., Patterson, C. C., and Boutron, C. F. (1996). History of Ancient Copper Smelting Pollution During Roman and Medieval Times Recorded in Greenland Ice. *Science* **272**, 246-249.
- Howe, E. G., and Petersen, U. (1992). Silver and Lead in the Late Prehistory of the Mantaro Valley, Peru. In "Archaeometry of pre-Columbian sites and artifacts." (D. A. Scott, and P. Meyers, Eds.), pp. 183-198. Getty Conservation Institute, Marina Del Rey, CA
- Isbell, W. H. (2004). Cultural Evolution in the Lake Titicaca Basin: Empirical Facts and Theoretical Expectations. *Reviews in Anthropology* **33**, 209-241.
- Jennings, J., and Craig, N. (2001). Politywide Analysis and Imperial Economy: The Relationship between Valley Political Complexity and Administrative Centers in the Wari Empire of the Central Andes. *Journal of Anthropological Archaeology* **20**, 479-502.
- Jones, J., and King, H. (2002). "Gold of the Americas." Metropolitan Museum of Art, New York.
- Kauppila, T. (2006). Sediment-Based Study of the Effects of Decreasing Mine Water Pollution on a Heavily Modified, Nutrient Enriched Lake. *Journal of Paleolimnology* **35**, 25-37.
- King, H. (2000). "Rain of the Moon: Silver in Ancient Peru." The Metropolitan Museum of Art, New York.
- Kober, B., Wessels, M., Bollhofer, A., and Mangini, A. (1999). Pb isotopes in sediments of Lake Constance, Central Europe constrain the heavy metal pathways and the pollution history of the catchment, the lake and the regional atmosphere. *Geochimica et Cosmochimica Acta* **63**, 1293-1303.
- Kolata, A. L. (1993). "The Tiwanaku: Portrait of an Andean Civilization." Blackwell, Oxford, UK.
- Kolata, A. L. (2003). "Tiwanaku and Its Hinterland: Archaeology and Paleoecology of an Andean Civilization." Smithsonian Institution Press, Washington, DC.
- Lechtman, H. (1976). A metallurgical site survey in the Peruvian Andes. *Journal of Field Archaeology* **3**, 1-42.
- Lechtman, H. (1979). Issues in Andean metallurgy. In "Pre-Columbian Metallurgy of South America." (E. P. Benson, Ed.). Dumbarton Oaks, Washington, DC.

- Lechtman, H. (1980). The Central Andes: Metallurgy without iron. *In* "The Coming Age of Iron." (T. A. Wertime, and J. D. Muhley, Eds.). Yale University Press, New Haven, CN.
- Lechtman, H. (1984). Andean Value Systems and the Development of Prehistoric Metallurgy. *Technology and Culture* **25**, 1-36.
- Lechtman, H. (1996). Arsenic Bronze: Dirty Copper or Chosen Alloy? *Journal of Field Archaeology* **23**, 477-514.
- Lechtman, H. (2002). Tiwanaku Period (Middle Horizon) Bronze Metallurgy in the Lake Titicaca Basin: A Preliminary Assessment. *In* "Tiwanaku and its Hinterland, Archaeology and Paleoecology of an Andean Civilization, Vol. II: Urban and Rural Archaeology." (A. L. Kolata, Ed.). Smithsonian Institution Press, Washington, DC.
- Lechtman, H. (2005). Arsenic Bronze at Pikillacta. *In* "Pikillacta: The Wari Empire in Cuzco." (G. F. McEwan, Ed.), pp. 131-146. University of Iowa Press, Iowa City.
- Lechtman, H., and Klein, S. (1999). The Production of Copper-Arsenic Alloys (Arsenic Bronze) by Cosemelting: Modern Experiment, Ancient Practice. *Journal of Archaeological Science* **26**, 497-526.
- Macfarlane, A., Marcet, T. C., Lehuray, A., and Peterson, U. (1990). Lead Isotope Provinces of the Central Andes Inferred from Ores and Crustal Rocks. *Economic Geology* **85**, 1857-1880.
- Martinez Cortizas, A., Garcia-Rodeja Gayoso, E., and Weiss, D. (2002). Peat bog archives of atmospheric metal deposition. *The Science of The Total Environment* **292**, 1-5.
- Monna, F., Petit, C., Guillaumet, J. P., Jouffroy-Bapicot, I., Blanchot, C., Dominik, J., Losno, R., Richard, H., Leveque, J., and Chateau, C. (2004). History and Environmental Impact of Mining Activity in Celtic Aeduan Territory Recorded in a Peat Bog (Morvan, France). *Environmental Science and Technology* **38**, 665-673.
- Moseley, M. (2001). "The Incas and Their Ancestors: The Archaeology of Peru." Thames and Hudson, New York.
- Mukasa, S. B., Vidal C., C. E., and Injoque-Espinoza, J. (1990). Pb Isotope Bearing on the Metallogenesis of Sulfide Ore Deposits in Central and Southern Peru. *Economic Geology* **85**, 1438-1446.
- Ng, A., and Patterson, C. C. (1982). Changes in lead and barium with time in California offshore basin sediments. *Geochimica et Cosmochimica Acta* **46**, 2307-2321.
- Norton, S. A., and Kahl, J. S. (1991). Progress in understanding the chemical stratigraphy of metals in lake sediments in relation to acidic precipitation. *Hydrobiologia* **214**, 77-84.
- Nriagu, J. O. (1994). Mercury pollution from the past mining of gold and silver in the Americas. *Science of the Total Environment* **149**, 167-181.
- Olsen Bruhns, K. (1994). "Ancient South America." Cambridge University Press, Cambridge.
- Outridge, P. M., Stern, G. A., Hamilton, P. B., Percival, J. B., McNeely, R., and Lockhart, W. L. (2005). Trace metal profiles in the varved sediment of an Arctic lake. *Geochimica et Cosmochimica Acta* **69**, 4881-4894.
- Owen, B. (1986). "The Role of Common Metal Objects in the Inka State." Unpublished M.A. thesis, University of California.
- Owen, B. (2005). Distant Colonies and Explosive Collapse: The Two Stages of the Tiwanaku Diaspora in the Osmore Drainage. *Latin American Antiquity* **16**, 45-80.
- Peterson, U. (1965a). Application of saturation (solubility) diagrams to problems in ore deposits. *Economic Geology* **60**, 853-893.

- Peterson, U. (1965b). Regional geology and major ore deposits of Central Peru. *Economic Geology* **85**, 1287-95.
- Purser, W. F. C. (1971). "Metal-mining in Peru, Past and Present." Praeger Publishers, New York.
- Reimer, P. J., Baillie, M. G. L., Bard, E., Bayliss, A., Beck, J. W., Bertrand, C. J. H., Blackwell, P. G., Buck, C. E., Burr, G. S., Cutler, K. B., Damon, P. E., Edwards, R. L., Fairbanks, R. G., Friedrich, M., Guilderson, T. P., Hogg, A. G., Hughen, K. A., Kromer, B., McCormac, G., Manning, S., Ramsey, C. B., Reimer, R. W., Remmele, S., Southon, J. R., Stuiver, M., Talamo, S., Taylor, F. W., van der Plicht, J., and Weyhenmeyer, C. E. (2004). IntCal04 Terrestrial Radiocarbon Age Calibration, 0–26 Cal Kyr BP *Radiocarbon* **46**, 1029-1058.
- Renberg, I., Brännvall, M. L., Bindler, R., and Emteryd, O. (2002). Stable lead isotopes and lake sediments—a useful combination for the study of atmospheric lead pollution history. *The Science of the Total Environment* **292**, 45-54.
- Renberg, I., Persson, M. W., and Emteryd, O. (1994). Pre-industrial atmospheric lead contamination detected in Swedish lake sediments. *Nature* **368**, 323-326.
- Rodman, A. O. (1992). Textiles and Ethnicity: Tiwanaku in San Pedro de Atacama, North Chile. *Latin American Antiquity* **3**, 346-340.
- Rosman, K. J. R., Chisholm, W., Boutron, C. F., Candelone, J. P., and Hong, S. (1994). Isotopic evidence to account for changes in the concentration of lead in Greenland snow between 1960 and 1988. *Geochimica et Cosmochimica Acta* **58**, 3265-3269.
- Sangster, D. F., Outridge, P. M., and Davis, W. J. (2000). Stable lead isotope characteristics of lead ore deposits of environmental significance. *Environmental Reviews* **8**, 115-147.
- Schreiber, K. J. (1992). "Wari Imperialism in Middle Horizon Peru." Museum of Anthropology, University of Michigan, Ann Arbor.
- Seltzer, G. O., and Hastorf, C. A. (1990). Climatic Change and its Effects on Prehispanic Agriculture in the Central Peruvian Andes. *Journal of Field Archaeology* **17**, 397-414.
- Shimada, I., and Griffin, J. A. (2005). Precious Metal Objects of the Middle Sicán. *Scientific American* **15**, 80-89.
- Shirahata, H., Elias, R. W., and Patterson, C. C. (1980). Chronological variations in concentrations and isotopic compositions of anthropogenic atmospheric lead in sediments of a remote subalpine pond. *Geochimica et Cosmochimica Acta* **44**, 149-162.
- Shotyk, W., Cheburkin, A. K., Appleby, P. G., Fankhauser, A., and Kramers, J. D. (1996). Two thousand years of atmospheric arsenic, antimony, and lead deposition recorded in an ombrotrophic peat bog profile, Jura Mountains, Switzerland. *Earth and Planetary Science Letters* **145**, 1-7.
- Stanish, C. (2002). Tiwanaku Political Economy. In "Andean Archaeology I: Variations in Sociopolitical Organization." (W. H. Isbell, and H. Silverman, Eds.), pp. 169-198. Kluwer Academic/Plenum, New York.
- Thompson, L. G., Mosley-Thompson, E., Bolzan, J. F., and Koci, B., R. (1985). A 1500-Year Record of Tropical Precipitation in Ice Cores from the Quelccaya Ice Cap, Peru. *Science* **229**, 971-973.
- Townsend, A. T., and Snape, I. (2002). The use of Pb isotope ratios determined by magnetic sector ICP-MS for tracing Pb pollution in marine sediments near Casey Station, East Antarctica. *Journal of Analytical Atomic Spectrometry* **17**, 922-928.

- Van Buren, M., and Mills, B. H. (2005). Huayrachinas and tocochimbo: traditional smelting technology of the southern Andes. *Latin American Antiquity* **16**, 2-23.
- Véron, A., Lambert, C. E., Isley, A., Linet, P., and Grousset, F. (1987). Evidence of recent lead pollution in deep north-east Atlantic sediments. *Nature* **326**, 278-281.
- Ward, H. J. (1961). The pyrite body and copper orebodies, Cerro de Pasco Mine, central Peru. *Economic Geology* **56**, 402-422.
- Williams, P. R. (2002). Rethinking disaster-induced collapse in the demise of the Andean highland states: Wari and Tiwanaku. *World Archaeology* **33**, 361-374.